

Large-Scale Structure and Gravitational Waves III: Tidal Effects

Fabian Schmidt,^{1,2} Enrico Pajer,³ and Matias Zaldarriaga⁴

¹*Max-Planck-Institute for Astrophysics, D-85748 Garching, Germany*

²*Department of Astrophysical Sciences, Princeton University, Princeton, NJ 08544, USA*

³*Department of Physics, Princeton University, Princeton, NJ 08544, USA*

⁴*Institute for Advanced Study, Princeton, NJ 08540, USA*

(Dated: November 6, 2018)

The leading locally observable effect of a long-wavelength metric perturbation corresponds to a tidal field. We derive the tidal field induced by scalar, vector, and tensor perturbations, and use second order perturbation theory to calculate the effect on the locally measured small-scale density fluctuations. For sub-horizon scalar perturbations, we recover the standard perturbation theory result (F_2 kernel). For tensor modes of wavenumber k_L , we find that effects persist for $k_L\tau \gg 1$, i.e. even long after the gravitational wave has entered the horizon and redshifted away, i.e. it is a “fossil” effect. We then use these results, combined with the “ruler perturbations” of [1], to predict the observed distortion of the small-scale matter correlation function induced by a long-wavelength tensor mode. We also estimate the observed signal in the B mode of the cosmic shear from a gravitational wave background, including both tidal (intrinsic alignment) and projection (lensing) effects. The non-vanishing tidal effect in the $k_L\tau \gg 1$ limit significantly increases the intrinsic alignment contribution to shear B modes, especially at low redshifts $z \lesssim 2$.

I. INTRODUCTION

Cosmological perturbation theory is a robust pillar on which our interpretation of cosmological observations rests. Although the linear results are by now part of textbook material, second and higher order effects have not yet been comprehensively computed. Given the ever increasing amount and precision of observations, many of these effects have already been or soon will be detected, providing strong motivation for a growing body of work (see [2–11] for recent developments).

While independent in linear perturbation theory, scalar, vector, and tensor modes are coupled at second order. This leads to interesting effects which have only recently been begun to be explored. While vector modes decay at linear order also on super horizon scales, tensors are conserved and might therefore have survived since the very early universe, thereby providing us with a unique opportunity to peek almost directly into those early stages of cosmological evolution. Specifically, a measurement of a scale-invariant background of gravitational waves would provide strong support for the inflationary paradigm, and tell us about the energy scale of inflation.

In this paper, we show that the leading locally observable effect of a long-wavelength perturbation k_L (be it scalar, vector, or tensor) on small-scale density perturbations with $k_S \gg k_L$ is given by an effective tidal field, and we derive the resulting contribution to the density field at second order. Our formalism thus captures any purely gravitational coupling at leading order in k_L/k_S . The most well-known case is a long-wavelength density (scalar) perturbation, whose effect on small-scale fluctuations is given by standard second-order perturbation theory (specifically the F_2 kernel). As a check of our formalism and computations, we re-derive this standard result. Our results are new for tidal fields of vector ori-

gin, which, to the best of our knowledge, have not been previously considered in the literature. For the case in which the tidal field is generated by gravitational waves (tensor modes), first estimates of the tidal effects were given in [12, 13]. More recently, a detailed computation has been presented in [14] assuming matter domination. Comparison with these previous works is in order. In [12], the anisotropy in the short-scale power spectrum was estimated to be of order $h_{ij}^{(0)} k_S^i k_S^j / k_S^2$, where $h_{ij}^{(0)}$ is the spatial metric perturbation at early times. Although this agrees with our final result and that of [14] up to factors of order one, it does not capture the time dependence of the effect which sheds light on the physical origin of the effect as we will see momentarily. In [13] it was roughly estimated that the “intrinsic” shape correlations of galaxies induced by tensor modes are proportional to the instantaneous amplitude of the tensor mode tidal field, while we will argue that it should be more accurately given by a certain time integral over the tidal field. Let us defer galaxy alignments for the moment and consider the anisotropy of small-scale density statistics. We reproduce the results of [14] in the matter dominated regime ($k_L \lesssim 0.01 h \text{Mpc}^{-1}$). However, we argue that a signal of comparable size will come from smaller scale tensor modes that entered the horizon during radiation domination. Our treatment of radiation domination neglects perturbations in radiation, which we will study in a separate publication. This additional effect will however not change the above conclusion. Let us stress that by dividing the effects into separately observable pieces as we will describe now, we believe our approach makes the physics of the tensor mode effects intuitive and transparent.

Before presenting our results, we briefly summarize our methodology. The purely gravitational effect of long wavelength metric perturbations on short scales can be captured in a convenient and physically transparent way

adopting a series of different coordinates [15]. Given some set of long-wavelength primordial metric perturbations $h(k_L)$, one can define *conformal Fermi Normal Coordinates* (FNC) at all times along any chosen timelike geodesic. In these local coordinates, the metric is FLRW along the central geodesic with all physical effects due to $h(k_L)$ being encoded in corrections to the metric at order $(\nabla\nabla h)x^2$. Results obtained in these coordinates have a clear physical interpretation as corresponding to what a local freely falling observer moving along the central geodesic would measure.

In the end, one is typically interested in how the perturbations $h(k_L)$ affect measurements by an observer far away, e.g. on Earth. This requires computing *projection effects*, which we define as the mapping from local FNC coordinates to the coordinates chosen by the observer. We will perform this mapping using the results of [1]. An advantage of this methodology is that all results at all points of the computation represent physical observables. This is to be contrasted with using global coordinates, in which case unphysical contributions from different parts of the computation need to cancel each other before the final observable result is obtained.

Our main result for tensor (and vector) perturbations can be summarized as follows. Given a primordial spatial metric perturbation¹ $h_{ij}^{(0)}$ at position \mathbf{x} (traceless by assumption) with comoving wavenumber k_L , the density field $\delta_{2,t}$ at conformal time τ is given in terms of the linear density field $\delta_{1,s}$ at the same time by

$$\begin{aligned} \delta_{2,t}(\mathbf{x}, \tau) & \quad (1) \\ & = h_{ij}^{(0)}(\mathbf{x}) \left[\alpha(k_L, \tau) \frac{\partial^i \partial^j}{\nabla^2} + \beta(k_L, \tau) x^i \partial^j \right] \delta_{1,s}(\mathbf{x}, \tau). \end{aligned}$$

The notation $\delta_{2,t}$ indicates that this is the correction to the linear density field induced at second order by vector and tensor modes (see Tab. I for a summary of our notation). Here the coefficients α , β are functions of the wavenumber k_L and conformal time τ . In particular, for $k_L\tau \ll 1$, i.e. when the long-wavelength modes are superhorizon, α and β go to zero as demanded by the equivalence principle. More interesting is the opposite limit $k_L\tau \gg 1$, when the tensor or vector mode has long entered the horizon and decayed. We will see that, despite what one might have expected, the coefficients α and β do not vanish in this limit but rather asymptote to constant values α_∞ , β_∞ . Thus, the small-scale density field preserves the knowledge of the primordial vector or tensor modes which have long decayed away. Such a feature was called *fossil effect* in [12], and we will adopt this name for the $k_L\tau \gg 1$ limit of the tidal effects. Notice that the fossil effect is generated at the time of horizon re-entry of the tensor or vector mode. For modes of observational interest, this happens at $z < 10^5$, much after

inflation and reheating. In this sense, although the size of the effect is proportional to the primordial tensor modes, the physical coupling between tensors and scalars that we discuss in this work is generated in the late universe.

The two terms in Eq. (1) correspond to different physical effects. The first term ($\propto \alpha$) indicates the effect of the tidal field on the evolution of small-scale fluctuations. The second term ($\propto \beta$) on the other hand encodes the effect of the displacement of matter by the long-wavelength tidal field. In other words, it is the effect of the tidal field on the mapping from Lagrangian to Eulerian positions.

The most obvious observational consequence of the effect described in Eq. (1) is an *anisotropic distortion of the local small-scale power spectrum*, whose fractional amplitude is given by

$$\begin{aligned} & \frac{P(\mathbf{k}_S, \tau | h_{ij}^{(0)})}{P_L(k_S, \tau)} - 1 \\ & = 2 \hat{k}_S^i \hat{k}_S^j h_{ij}^{(0)} \left[\alpha(k_L, \tau) - \beta(k_L, \tau) \frac{d \ln P_L(k_S, \tau)}{d \ln k_S} \right]. \end{aligned} \quad (2)$$

Given that we consider the regime $k_L/k_S \ll 1$, this expression can then be used to derive the contribution to the tensor-scalar-scalar bispectrum $\langle h_{ij}^{(0)}(\mathbf{k}_L) \delta(\mathbf{k}_S) \delta(\mathbf{k}_S) \rangle$ in the squeezed limit. Of course, this bispectrum is only accessible observationally if one has an independent measurement of the vector or tensor modes. Alternatively, if no independent estimate of $h_{ij}^{(0)}$ is available, Eq. (2) also describes a specific, anisotropic contribution to the collapsed limit of the four-point function of the density field [16], which can be measured without any external data sets. The specific case studied by [16] was the 21cm emission at high redshifts. However, the same idea, applied to long-wavelength scalar tidal fields, also underlies the tidal field reconstruction of [17].

Another probe of anisotropic small-scale fluctuations is the *alignment of dark matter halos*, that are known to orient along long-wavelength tidal fields, and that in turn influence the orientations of galaxies within them [18–20]. This can be observed through the shapes of galaxy images, as measured in large area weak lensing shear surveys. The preferential alignment of galaxy images with large-scale tidal fields is known as *intrinsic alignments*. Schmidt and Jeong [13] were the first to point out that tensor modes are also expected to contribute to intrinsic alignments. As shown there, the observed galaxy shape correlations induced by tensor modes are in fact expected to be dominated by the alignment contribution. The reason for this is that the tensor-mode lensing effect (part of the projection effects discussed above) is strongly suppressed as the propagating gravitational waves fail to produce a coherent deflection along the light cone as scalar perturbations do.

However, the estimates of the alignment effect in [13] did not take into account the qualitatively different evolution with time of tensor with respect to scalar tidal fields. Specifically, they assumed that the alignment is proportional to the instantaneous tidal field at the time

¹ For vector perturbations, we here assume instantaneous generation at some initial time.

Symbol	Relation	Meaning
\mathcal{H}	$= a'/a = aH$	comoving Hubble scale
δ	$= \rho_m(\mathbf{x})/\bar{\rho}_m - 1$	matter density perturbation
Φ_s	Eq. (5)	Newtonian gauge potential in absence of tidal field
t_{ij}, T	$t_{ij}(\mathbf{0}; \tau) = T(k_L, \tau) t_{ij}^{(0)}(\mathbf{0})$	tidal field t_{ij} and its transfer function T
α, β, γ	Eq. (39)	functions of k and τ
$V, F, D_{\sigma_1}, D_{\sigma_2}$	Eq. (21), Eq. (30), Eq. (31), Eq. (32)	functions of k and τ
\mathbf{s}	$\mathbf{x}(\mathbf{q}, \tau) = \mathbf{q} + \mathbf{s}(\mathbf{q}, \tau)$	Lagrangian displacement vector
\mathbf{q}	$\mathbf{x}(\mathbf{q}, \tau) = \mathbf{q} + \mathbf{s}(\mathbf{q}, \tau)$	Lagrangian coordinate
\mathbf{x}	$\mathbf{x}(\mathbf{q}, \tau) = \mathbf{q} + \mathbf{s}(\mathbf{q}, \tau)$	Eulerian coordinate
u^i	Eq. (B1)	peculiar velocity
θ	$= \partial_i u^i$	peculiar velocity divergence
subscripts 1, 2, ...	$\delta = \delta_1 + \delta_2 + \dots$	(matter) perturbations at linear, second, ... order
subscripts t or s	$\delta_1 = \delta_{1,s} + \delta_{1,t}$	contributions at 0'th and first order in the tidal field
subscripts L or S	$k_L \ll k_S$	Long L and Short S wavelengths
superscript (0)	$h_{ij}^{(0)} = h_{ij}(\tau_0)$	quantity evaluated at "initial" time τ_0

TABLE I: Symbols used in the paper.

of observation of the galaxy. On the other hand, here we found, in agreement with [14], that the tidal effect on small-scale fluctuations comes instead from a time integral over the past history of the tensor mode that peaks at horizon crossing $k_L \simeq \mathcal{H}$ but remains constant afterwards. In Sec. VII of this paper, we use these results to provide a more accurate estimate of the intrinsic alignment by tensor modes. We find a shear B-mode power spectrum of $l(l+1)C_\gamma^{BB}(l)/2\pi \sim \text{few} \times 10^{-12}$ over a wide range of scales and redshifts (see Fig. 4).

The remainder of the paper derives the coefficient functions α and β , and presents these applications in more detail. The outline of the paper is as follows. In Sec. II we review Fermi Normal Coordinates (FNC) and their conformal analog ($\overline{\text{FNC}}$) introduced in [15] (leaving details to App. A) and derive a general expression for the local tidal field. In Sec. III we solve for the effect of the tidal field on short scale density fluctuations using Lagrangian Perturbation Theory (the equivalent Eulerian derivation can be found in App. B). We give explicit applications of our general results to long-wavelength scalar, vector and tensor perturbations in Sec. IV and Sec. V. We discuss projection effects and the distortion of small-scale correlations observed on Earth in Sec. VI. Finally, in Sec. VII we derive the implications of our results for lensing shear surveys.

Our notation is summarized in Tab. I. For our numerical results, we adopt a flat Λ CDM cosmology with $\Omega_{m0} = 1 - \Omega_{\Lambda 0} = 0.3$ and $h = 0.72$.

II. FERMI NORMAL COORDINATES

Our framework for the computation of gravitational tidal effects is the conformal Fermi normal coordinate ($\overline{\text{FNC}}$) frame, which was first introduced in Pajer et al.

[15] and which we review in this section.

Consider a perturbed FRW metric given by

$$g_{\mu\nu}(\tau, \mathbf{x}) = a(\tau)^2 [\eta_{\mu\nu} + h_{\mu\nu}(\tau, \mathbf{x})] , \quad (3)$$

with $\eta_{\mu\nu}$ the mostly positive Minkowski-space metric and $h_{\mu\nu} \ll 1$ some set of small perturbations. We want now to study the effect of the interactions between long (k_L) and short (k_S) wavelength perturbations in h , assuming $k_L \ll k_S$. For this purpose we consider a region around the timelike geodesic of a comoving observer governed by the metric Eq. (3), with approximate size k_S^{-1} on a certain spatial slice around the geodesic. We can then construct a coordinate frame $\{\bar{x}_F^\mu\}$ with spatial origin corresponding to this central geodesic in which the metric is Friedmann-Robertson-Walker along the central geodesic, with corrections going as the spatial distance from the geodesic squared (the explicit form is given in [15], see also App. A) *at all times* \bar{x}_F^0

$$g_{\mu\nu}^F = a^2(x^0[\bar{x}_F^0]) [\eta_{\mu\nu} + \mathcal{O}([\bar{x}_F^i]^2)] . \quad (4)$$

Note that these coordinates are not globally valid, but apply in a "spaghetti-shaped" region of spacetime around the central geodesic. We call the frame described by the coordinates $\{\bar{x}_F^\mu\}$ the *conformal* Fermi Normal Coordinate frame ($\overline{\text{FNC}}$), as it is a generalization of the Fermi Normal Coordinates (FNC) first introduced by [21] (and recently applied in cosmology in [1, 13, 22]). We give here a brief overview of its properties and refer the reader to [15] for further details. When the size $\sim k_S^{-1}$ of the region considered is much smaller than the horizon, then we can do a further simple coordinate transformation to recover the standard FNC. However, unlike the standard FNC, $\overline{\text{FNC}}$ are also applicable if the region considered is superhorizon.

In case of the standard FNC, the $\mathcal{O}(x_F^2)$ corrections are given by the Riemann tensor evaluated along the central geodesic. For the metric Eq. (3) (at linear order in h), this includes terms of order H^2 , $H\nabla h$, and $\nabla\nabla h$ (here ∇ stands for either a space or time derivative). As we show in App. A, the $\mathcal{O}(\bar{x}_F^2)$ corrections in $\overline{\text{FNC}}$ on the other hand come from two sources: first, there are contributions of order $\nabla\nabla h$ from the Riemann tensor of the *conformal* metric $\eta_{\mu\nu} + h_{\mu\nu}$, which agree with the corresponding terms in FNC (up to factors of a from the leading order relation $x_F^i = a\bar{x}_F^i$ between spatial FNC and $\overline{\text{FNC}}$). Second, there are terms of order $H\nabla h$ which enter through the a^2 prefactor due to the transformation of the time coordinate. Again, these agree with the terms of the same type in FNC. Finally, the $\mathcal{O}(H^2 x_F^2)$ terms disappear in $\overline{\text{FNC}}$, since we have explicitly kept the a^2 prefactor.

Thus, the $\overline{\text{FNC}}$ correspond to the natural *comoving* coordinates an observer moving along the central geodesic would choose. In fact, the coordinates chosen to interpret cosmological observations from Earth are essentially $\overline{\text{FNC}}$ constructed for the geodesic of the Solar System and with the size of the patch given by our current Hubble horizon, thereby removing effects of all super-horizon modes $k_L < H_0$, where again k_L is the *comoving* wavenumber of the long-wavelength perturbation. As mentioned above, the advantage of the $\overline{\text{FNC}}$ frame over FNC is that the corrections to the FRW metric are always of order $(\bar{x}_F k_L)^2$ [so in case of the FNC around Earth, the parameter is $(k_L H_0)^2$]. This allows one to follow the given region around the central geodesic back to early times where it was larger than the horizon H^{-1} (at which point the regular FNC become invalid). The $\overline{\text{FNC}}$ frame is useful for studying the gravitational interaction of perturbations in cosmology whenever there is a hierarchy between long and short modes, so that the effect of the long modes can be studied neglecting corrections of higher order in k_L/k_S .

A. Non-relativistic limit

Note that since we consider scalar² perturbations that are much smaller in scale than tensor perturbations $k_S \gg k_L$, and since the effect of the latter only becomes relevant as $k_L \gtrsim \mathcal{H}$, for all practical purposes we can restrict our analysis to when the short scalar fluctuations are well within the horizon, $k_S \gg \mathcal{H}$. Additionally, in this work we will restrict ourselves to the dynamics of non-relativistic matter. These two assumptions allow us to use the standard pseudo-Newtonian limit usually adopted in the theory of large-scale structure to describe

the gravitational dynamics on short scales.

Throughout, we neglect the effect of perturbations in the radiation component, which is not correct in general: radiation interacts gravitationally with matter at all times. Also, before recombination, radiation couples tightly to baryons. There are two regimes in which we can neglect the effect of radiation on matter. The first is during matter domination, i.e. for $a \gg a_{\text{eq}} = \Omega_{r0}/\Omega_{m0}$ (and hence after recombination) when the energy density of radiation has redshifted away and its gravitational coupling with matter is very small. The second is during radiation domination on scales smaller than the dissipation scale, where the perturbations in the electron-baryon-photon fluid are completely erased. Hence our results will be applicable in these two regimes. On the other hand, the scales that enter during radiation domination but are larger than the dissipation scale are quite interesting observationally, and deserve a separate study with a full relativistic treatment. We defer this to future work.

Consider objects in the vicinity of the central geodesic around which the $\overline{\text{FNC}}$ are constructed. If these objects are slow moving, i.e. if their velocities relative to that of the central geodesic are much smaller than the speed of light, then their dynamics are governed up to order v/c by g_{00}^F . In the following, we will assume that in global coordinates $h_{0i} = 0$, which applies to vector and scalar perturbations in popular gauges as well as tensor perturbations. In this case, g_{00}^F is given by (see App. A)

$$g_{00}^F = -a_F^2(\bar{\tau}_F) \left[1 + 2\Phi_s(\mathbf{x}, \bar{\tau}_F) - t_{ij}(\bar{\tau}_F) \bar{x}_F^i \bar{x}_F^j \right] \quad (5)$$

$$t_{ij}(\bar{\tau}_F) = \frac{1}{2} \left[a^{-1}(ah'_{ij})' + h_{00,ij} \right]. \quad (6)$$

Here, and throughout, primed denote derivatives with respect to τ . In Eq. (6), all occurrences of h are evaluated at a given proper time $\bar{\tau}_F$ along the central geodesic (i.e. at $\bar{\mathbf{x}}_F = 0$ in $\overline{\text{FNC}}$). a_F is the locally measured scale factor given by

$$a_F(\bar{\tau}_F) \equiv a(\tau(\bar{\tau}_F, \mathbf{0})) = a \left(\bar{\tau}_F + \frac{1}{2} \int^{\bar{\tau}_F} h_{00}(\mathbf{0}, \tau) d\tau \right). \quad (7)$$

The apparent unphysical dependence on a metric perturbation h_{00} (without any derivative) is simply because we are referring to an unobservable “background” scale factor $a(\tau)$ here. As discussed in more detail in App. A, this corresponds to an unobservable shift in the time coordinate. What *is* observable is the different proper time $\bar{\tau}_F$ of different regions on a constant-observed-redshift surface. This is part of the “projection effects” we will discuss in Sec. VIA.

There are two contributions to g_{00}^F : the first, Φ_s is the potential sourced by the small-scale scalar perturbations. The second, t_{ij} , is the tidal tensor induced by the long-wavelength metric perturbations. Note that t_{ij} has dimension $1/\text{length}^2$. We will work to linear order in

² The framework of the previous section is valid to study any type of small scale perturbations but in this paper we will focus on short *scalar* perturbations.

t_{ij} throughout. Note that we allow for a non-zero trace component t_i^i , which will permit us to consider a long-wavelength density perturbation in addition to vectors and tensors. There are corrections to Eq. (5) of order $(\bar{x}_F^i)^3$ which we neglect as they are suppressed by k_L/k_S .

The effect of tensor and, for common gauges such as Newtonian and synchronous gauges, that of vector modes is encoded in the h_{ij} contribution to t_{ij} . This contribution agrees with that derived in [13], taking into account that the tidal field in the latter paper is given in terms of physical coordinates $\mathbf{r}_F = a\bar{\mathbf{x}}_F$. We see that in order to have an effect, these modes have to evolve in time; specifically, superhorizon modes which are conserved will have no effect. On the other hand, scalar long-wavelength perturbations are encoded by the $h_{00} = -2\Phi_L$ contribution, where Φ_L is the long-wavelength potential perturbation in Newtonian gauge. Note that the tidal effect is proportional to the second *spatial* derivative of h_{00} : this reflects the fact that spatially constant and pure-gradient potential perturbations cannot have an observable impact by way of the equivalence principle.

In the following, we will work exclusively in the $\overline{\text{FNC}}$ frame. Therefore we simplify the notation in what follows:

$$\begin{aligned}\bar{x}_F^0 &\rightarrow \tau \\ \bar{x}_F^i &\rightarrow x^i \\ a_F &\rightarrow a.\end{aligned}\quad (8)$$

By separating the linearized Einstein equations into long- and short-wavelength parts and transforming the short-wavelength part to $\overline{\text{FNC}}$, one can show that up to corrections of order k_L/k_S , the small-scale potential Φ_s satisfies the standard Poisson equation in comoving coordinates,

$$\nabla^2 \Phi_s = 4\pi G a^2 \delta \rho = \frac{3}{2} \Omega_{m0} H_0^2 a^{-1} \delta = \frac{3}{2} \Omega_m(\tau) \mathcal{H}^2 \delta. \quad (9)$$

where G is Newton's constant, $\mathcal{H} = a'/a$, ρ is the matter density with homogenous average $\bar{\rho}$ and contrast $\delta \equiv \delta\rho/\bar{\rho} - 1$.

We define a transfer function $T(k_L, \tau)$ of the tidal field as follows,

$$t_{ij}(\mathbf{0}; \tau) = T(k_L, \tau) t_{ij}^{(0)}(\mathbf{0}), \quad (10)$$

which in general depends on the wavenumber k_L of the long-wavelength perturbation. We will give the transfer function explicitly later on when dealing with the scalar and tensor tidal fields separately. In the following, we will often suppress the argument k_L as it does not enter in the derivation otherwise. Throughout, we will assume that the source term for the second order density goes to zero at early times, i.e. $a(\tau)t_{ij}(\tau) \xrightarrow{\tau \rightarrow 0} 0$; more specifically, we assume that the small-scale fluctuations have settled into the growing mode by the time $a(\tau)t_{ij}(\tau)$ becomes non-negligible. This again is only valid if the wavelength of the small-scale fluctuations is sufficiently smaller than that of the tidal field.

III. LAGRANGIAN DERIVATION OF TIDAL EFFECTS

In this section, we derive the effects of the external field on small-scale density perturbations using the Lagrangian approach. A Eulerian derivation which arrives at the same result is given in App. B. For simplicity, we will assume an Einstein-de Sitter Universe in this section. This is applicable to external tidal fields which become relevant during matter domination, e.g. those induced by long-wavelength modes that enter the horizon during matter domination, i.e. with wave numbers $H_0^{-1} \ll k_L < k_{\text{eq}}$. We extend the derivation to include tidal fields that become relevant during radiation domination and Λ domination in Sec. V C.

The comoving Eulerian coordinate \mathbf{x} at conformal time τ is related to the Lagrangian coordinate \mathbf{q} by the displacement \mathbf{s} ,

$$\mathbf{x}(\mathbf{q}, \tau) = \mathbf{q} + \mathbf{s}(\mathbf{q}, \tau). \quad (11)$$

In Lagrangian perturbation theory (LPT), we adopt the single-stream approximation, in which case the Eulerian fractional matter overdensity $\delta(\mathbf{x}, \tau)$ is given by

$$\delta[\mathbf{x}(\mathbf{q}, \tau), \tau] = |\mathbf{1} + \mathbf{M}(\mathbf{q}, \tau)|^{-1} - 1, \quad (12)$$

where \mathbf{M}_{ij} is the deformation tensor,

$$\mathbf{M}_{ij}(\mathbf{q}, \tau) = \frac{\partial}{\partial q^i} s^j(\mathbf{q}, \tau). \quad (13)$$

Note that $\partial_q^i = \partial_x^i + \mathbf{M}_j^i \partial_q^j$. The evolution equation for \mathbf{s} is simply the equation of motion of a particle in comoving units,

$$s'^{i'}(\mathbf{q}, \tau) + \mathcal{H} s'^i(\mathbf{q}, \tau) = -\partial_x^i \left[\Phi_s(\mathbf{x}) + \frac{1}{2} t_{kl} x^k x^l \right]_{\mathbf{x}(\mathbf{q}, \tau)}, \quad (14)$$

where primes denote derivatives with respect to conformal time τ . Using Eq. (12), the Poisson equation Eq. (9) becomes at second order

$$\begin{aligned}\nabla_x^2 \Phi_s(\mathbf{x}(\mathbf{q})) &= \frac{3}{2} \Omega_m \mathcal{H}^2 \delta(\mathbf{x}(\mathbf{q})) \\ &= \frac{3}{2} \Omega_m \mathcal{H}^2 \left[-\text{Tr} \mathbf{M} + \frac{1}{2} ((\text{Tr} \mathbf{M})^2 + \text{Tr}(\mathbf{M} \cdot \mathbf{M})) \right. \\ &\quad \left. + \mathcal{O}((\mathbf{M})^3) \right]_{\mathbf{q}}.\end{aligned}\quad (15)$$

We are interested in the leading effect of t_{ij} on the density in Eulerian space Eq. (12). For this, we decompose the displacement as

$$\mathbf{s} = \mathbf{s}_s + \mathbf{s}_t, \quad (16)$$

where \mathbf{s}_s is the scalar contribution which remains when setting t_{ij} to zero. Correspondingly, we will use \mathbf{M}_s , \mathbf{M}_t .

We will further perform a perturbative expansion in \mathbf{s} . Specifically, we consider the linear displacement, which uniquely separates into scalar and tensor pieces $\mathbf{s}_{1,s}$, $\mathbf{s}_{1,t}$, and the quadratic mixed contribution from the coupling of \mathbf{s}_s and \mathbf{s}_t , denoted as $\mathbf{s}_{2,t}$ (the contributions of order $(s_{1,s})^2$ lead to the standard second order LPT result). Without loss of generality, we set $\mathbf{s}_{1,s}(\mathbf{q} = 0, \tau) = \mathbf{0} = \mathbf{s}_{1,t}(\mathbf{q} = 0, \tau)$ at some time of interest τ , so that *at linear order* the origin coincides in both Eulerian and Lagrangian coordinates.

A. Linear solutions

The linearized version of Eq. (14) becomes, separated into scalar and tensor parts,

$$\begin{aligned} s_{1,s}^{\prime\prime i}(\mathbf{q}, \tau) + \mathcal{H}s_{1,s}^{\prime i}(\mathbf{q}, \tau) &= \frac{3}{2}\mathcal{H}^2 \frac{\partial_q^i}{\nabla_q^2} \partial_{qj} s_{1,s}^j(\mathbf{q}, \tau) \\ s_{1,t}^{\prime\prime i}(\mathbf{q}, \tau) + \mathcal{H}s_{1,t}^{\prime i}(\mathbf{q}, \tau) &= -\frac{1}{2}\partial_q^i [t_{kl}(\tau)q^k q^l]. \end{aligned} \quad (17)$$

Since this is at linear order, we have set $\mathbf{x} = \mathbf{q}$. Assuming only the growing mode is present in the initial conditions, the first equation can be integrated to give

$$s_{1,s}^i(\mathbf{q}, \tau) = -\frac{\partial_q^i}{\nabla_q^2} \delta_{1,s}(\mathbf{q}, \tau) = -a(\tau) \frac{\partial_q^i}{\nabla_q^2} \delta_{1,s}(\mathbf{q}, \tau_0), \quad (18)$$

where $a(\tau_0) = 1$. The equation for $s_{1,t}^i$, rewritten as

$$(\tau^2 s_{1,t}^i)' = -\tau^2 T(\tau) t^{(0)i}{}_k q^k, \quad (19)$$

can be integrated to give

$$s_{1,t}^i(\mathbf{q}, \tau) = -F(\tau) t^{(0)i}{}_k q^k \quad (20)$$

$$F(\tau) \equiv \int_0^\tau \frac{d\tau'}{a(\tau')} \int_0^{\tau'} d\tau'' a(\tau'') T(\tau''). \quad (21)$$

Note that

$$T(\tau) = \frac{1}{a(\tau)} [a F'(\tau)]', \quad (22)$$

and that Eqs. (20)–(21) are valid for a general expansion history. In parallel with the linear scalar density $\delta_{1,s}$, we define

$$\delta_{1,t}(\mathbf{q}, \tau) = -\partial_{q^i} s_{1,t}^i(\tau) = F(\tau) t^{(0)i}{}_i. \quad (23)$$

If $t_k^k = 0$, $\text{Tr } \mathbf{M}_{1,t} = 0$ and there is no first-order contribution to the density ($\delta_{1,t} = 0$) as expected.

B. Second-order solution

The equation for the second-order displacement $s_{2,t}$ is obtained by collecting all second-order pieces from the

right-hand side of Eq. (14). As described above, we will only consider the coupling of $s_{1,s}$ with $s_{1,t}$.

Taking the divergence with respect to \mathbf{q} of the equation for \mathbf{s} [Eq. (14)] yields

$$\begin{aligned} \sigma'' + \mathcal{H}\sigma' &= -\nabla_x^2 \Phi_s - \mathbf{M}_{ij} \partial_x^i \partial_x^j \Phi_s \\ &\quad - \mathbf{M}_{ij} \partial_x^i \partial_x^j \left[\frac{1}{2} t_{kl} x^k x^l \right], \end{aligned} \quad (24)$$

where $\sigma = \partial_{q^i} s^i$ and the r.h.s. is evaluated at $\mathbf{x}(\mathbf{q})$. Inserting the Poisson equation at second order [Eq. (15)], writing $\mathbf{M} = \mathbf{M}_s + \mathbf{M}_t$, and subtracting the equation for $\mathbf{s}_{1,t}$ [Eq. (17)] leads to the following equation for $\sigma_{2,t}$:

$$\begin{aligned} \sigma_{2,t}'' + \mathcal{H}\sigma_{2,t}' &= \frac{3}{2}\Omega_m \mathcal{H}^2 \text{Tr } \mathbf{M}_{2,t} \\ &\quad - \frac{3}{2}\Omega_m \mathcal{H}^2 \text{Tr } \mathbf{M}_{1,s} \text{Tr } \mathbf{M}_{1,t} - \mathbf{M}_{1,s}^{ij} t_{ij}, \end{aligned} \quad (25)$$

where on the r.h.s. all contributions are evaluated at \mathbf{q} . Note that the second term in Eq. (24) has canceled with the term $\propto \text{Tr } \mathbf{M}_s \cdot \mathbf{M}_t$ from the second-order density. We obtain

$$\begin{aligned} \sigma_{2,t}'' + \mathcal{H}\sigma_{2,t}' &- \frac{3}{2}\Omega_m \mathcal{H}^2 \sigma_{2,t} \\ &= -\frac{3}{2}\Omega_m \mathcal{H}^2 \delta_{1,s} \delta_{1,t} \Big|_{\mathbf{q}, \tau} + \left(\frac{\partial^i \partial^j}{\nabla^2} \delta_{1,s} \right)_{\mathbf{q}, \tau} t_{ij}(\tau). \end{aligned} \quad (26)$$

Specializing to Einstein-de Sitter, the previous equation becomes

$$\begin{aligned} \sigma_{2,t}''(\mathbf{q}, \tau) + \frac{2}{\tau} \sigma_{2,t}'(\mathbf{q}, \tau) - \frac{6}{\tau^2} \sigma_{2,t}(\mathbf{q}, \tau) &= \Sigma(\mathbf{q}, \tau) \\ \Sigma(\mathbf{q}, \tau) &= -\frac{3}{2} H_0^2 a(\tau) \delta_{1,s}(\mathbf{q}, \tau_0) F(\tau) t^{(0)i}{}_i \\ &\quad + a(\tau) T(\tau) \left(\frac{\partial^i \partial^j}{\nabla^2} \delta_{1,s}(\mathbf{q}, \tau_0) \right) t_{ij}^{(0)}. \end{aligned} \quad (27)$$

The growing and decaying modes of this equation correspond to $\sigma_{2,t} \propto \tau^2$ and $\sigma_{2,t} \propto \tau^{-3}$, respectively, and the solution is

$$\sigma_{2,t}(\mathbf{q}, \tau) = \int_0^\tau d\tau' \frac{1}{5} \left[\frac{\tau^2}{\tau'} - \frac{\tau'^4}{\tau^3} \right] \Sigma(\mathbf{q}, \tau'). \quad (28)$$

By assumption (see the last paragraph of Sec. II A), $\Sigma(\mathbf{q}, \tau) \rightarrow 0$ as $\tau \rightarrow 0$, and we have fixed the boundary conditions so that both $\sigma_{2,t}$ and $\sigma_{2,t}'$ vanish in this limit as well. We then obtain

$$\begin{aligned} \sigma_{2,t}(\mathbf{q}, \tau) &= D_{\sigma 1}(\tau) \left(\frac{\partial^i \partial^j}{\nabla^2} \delta_{1,s}(\mathbf{q}, \tau) \right) t_{ij}^{(0)} \\ &\quad - \frac{3}{2} D_{\sigma 2}(\tau) \delta_{1,s}(\mathbf{q}, \tau) t_i^{(0)i}, \end{aligned} \quad (29)$$

where the coefficient functions are given by

$$V(\tau) \equiv \int_0^\tau d\tau' \frac{\tau'^5}{\tau^5} F'(\tau') \quad (30)$$

$$\begin{aligned} D_{\sigma_1}(\tau) &\equiv \frac{1}{a(\tau)} \int_0^\tau d\tau' \frac{1}{5} \left[\frac{\tau^2}{\tau'} - \frac{\tau'^4}{\tau^3} \right] a(\tau') T(\tau') \\ &= \frac{1}{5} \{F(\tau) + 4V(\tau)\} \end{aligned} \quad (31)$$

$$D_{\sigma_2}(\tau) \equiv \frac{H_0^2}{a(\tau)} \int_0^\tau d\tau' \frac{1}{5} \left[\frac{\tau^2}{\tau'} - \frac{\tau'^4}{\tau^3} \right] F(\tau'). \quad (32)$$

Let us now derive the *Eulerian* density in the presence of t_{ij} . This is defined as

$$\delta_t(\mathbf{x}) = \delta(\mathbf{x}) - \delta(\mathbf{x})|_{t_{ij}=0}. \quad (33)$$

Using Eq. (12), we have

$$\begin{aligned} \delta_t(\mathbf{x}(\mathbf{q})) &= \delta_{1,t}(\mathbf{q}) + \delta_{2,t}(\mathbf{x}(\mathbf{q})) \\ &= \delta_{1,t}(\mathbf{q}) - \sigma_{2,t}(\mathbf{q}) + \delta_{1,t}(\mathbf{q})\delta_{1,s}(\mathbf{q}) + \text{Tr}(\mathbf{M}_{1,s} \cdot \mathbf{M}_{1,t})_{\mathbf{q}}. \end{aligned}$$

However, there is a further subtlety in Eq. (33): we want to compare the overdensities at the same *Eulerian* position \mathbf{x} . The *Lagrangian* coordinate that corresponds to this position is different for $t_{ij} \neq 0$ and $t_{ij} = 0$. More precisely, we have (at linear order which suffices for this purpose)

$$\mathbf{x} = \mathbf{q} + \mathbf{s}_{1,s} + \mathbf{s}_{1,t}, \quad (34)$$

whereas $\delta_{1,s}$ as defined here gives the density at

$$\mathbf{x}_s = \mathbf{q} + \mathbf{s}_{1,s} = \mathbf{x} - \mathbf{s}_{1,t}. \quad (35)$$

Thus, the contribution to the Eulerian density by tensor modes is

$$\begin{aligned} \delta_t(\mathbf{x}, \tau) &= \delta_{1,t}(\mathbf{x}) - \sigma_{2,t}(\mathbf{x}) + \delta_{1,t}(\mathbf{x})\delta_{1,s}(\mathbf{x}) \\ &\quad + \text{Tr}(\mathbf{M}_{1,s} \cdot \mathbf{M}_{1,t})_{\mathbf{x}} - (\mathbf{x} - \mathbf{x}_s) \cdot \nabla_{\mathbf{q}} \delta_{1,s}(\mathbf{q}) \Big|_{\mathbf{x}} \\ &= \delta_{1,t}(\mathbf{x}) - \sigma_{2,t}(\mathbf{x}) + \delta_{1,t}(\mathbf{x})\delta_{1,s}(\mathbf{x}) \\ &\quad + \text{Tr}(\mathbf{M}_{1,s} \cdot \mathbf{M}_{1,t})_{\mathbf{x}} - s_{1,t}^i(\mathbf{x}) \partial_{q_i} \delta_{1,s}(\mathbf{x}). \end{aligned} \quad (36)$$

Note that we can replace \mathbf{q} with \mathbf{x} at this order. Inserting the expressions derived above, we obtain for the second order contribution

$$\begin{aligned} \delta_{2,t}(\mathbf{x}, \tau) &= t_{ij}^{(0)} \left[-D_{\sigma_1}(\tau) \frac{\partial^i \partial^j}{\nabla^2} + \frac{3}{2} \delta^{ij} D_{\sigma_2}(\tau) \right. \\ &\quad \left. + F(\tau) \left\{ \delta^{ij} + \frac{\partial^i \partial^j}{\nabla^2} + x^i \partial^j \right\} \right] \delta_{1,s}(\mathbf{x}, \tau). \end{aligned} \quad (37)$$

To recap, the first two terms here come from the modified second-order evolution of the scalar fluctuations, due to the presence of the external tidal field proper (first term) and the additional contribution to the matter density (second term). The next two terms are due to

the non-linear relation between displacement and density, which entails a coupling of the linear displacements due to small-scale scalar and external tidal displacements. Finally, the last term is directly proportional to the displacement by the external tidal field, and encodes the fact that we evaluate the small-scale perturbations at different relative (*Eulerian*) positions than we would have in the absence of t_{ij} .

We can now bring Eq. (37) into the form of Eq. (1) in Sec. I:

$$\begin{aligned} \delta_{2,t}(\mathbf{x}, \tau) &= t_{ij}^{(0)}(\mathbf{x}) \left[\alpha(\tau) \frac{\partial^i \partial^j}{\nabla^2} + \beta(\tau) x^i \partial^j + \gamma(\tau) \delta^{ij} \right] \delta_{1,s}(\mathbf{x}, \tau), \end{aligned} \quad (38)$$

where

$$\begin{aligned} \alpha(\tau) &= \frac{4}{5} \{F(\tau) - V(\tau)\} \\ \beta(\tau) &= F(\tau) \\ \gamma(\tau) &= \frac{3}{2} D_{\sigma_2}(\tau) + F(\tau). \end{aligned} \quad (39)$$

Again, there is a dependence on k_L which we have not written here that enters through the transfer function in Eq. (21) and Eqs. (30)–(32).

IV. SCALAR TIDAL FIELD

In this section, we consider a tidal field t_{ij} induced by a long-wavelength density perturbation $\delta_{1,L}$. In principle we could perform this computation for any $k_L \ll k_S$. On the other hand, our goal is to make contact with standard results, thus providing a non-trivial check of our formulae. Therefore we will assume to be in matter domination and that the long mode is well inside the horizon, namely $k_L \gg \mathcal{H}$. In this case, Eq. (38) should reduce to the standard expression (F_2 kernel of [23]) for the second order density perturbation in the limit that one mode is much longer than the other.

Before discussing the detailed calculation it is useful to present a heuristic but intuitive derivation of the main result of this section. We want to predict the structure of the second order density field δ_2 . Up to a potentially time-dependent factor, this is the same as the quadratic source terms in the Eulerian equation of motion for δ , Eq. (B12). To avoid proliferation of ∇^{-2} it is convenient to use the Newtonian potential and its derivatives as fundamental building block $\Phi \sim (\mathcal{H}^2/k^2) \delta$, instead of δ itself. Then, we should write all possible second order terms using just Φ and spatial derivatives, since time derivatives are very small during matter domination (zero in exact EdS). First we notice that Φ must appear with at least one derivative (a constant Φ cannot lead to any physical effect); the term with one derivative

contains a locally-unobservable uniform acceleration or bulk flow as we will discuss below. Second, since δ is a scalar we need to have an even total number of derivatives (lest we are left with uncontracted indices). The lowest number of derivatives is then two but the term $\partial_i \Phi \partial_i \Phi$ cannot appear because the equation for δ has an additional spatial derivative with respect to the Euler equation (conservation of momentum in Eq. (B3)) where each Φ should appear with at least one spatial derivative. Hence the allowed second order terms have at least four derivatives:

$$\partial_i \partial_j \Phi \partial_i \partial_j \Phi, \quad \partial^2 \Phi \partial^2 \Phi, \quad \text{and} \quad \partial_i \Phi \partial_i \partial^2 \Phi. \quad (40)$$

Terms with a higher number of spatial derivatives are suppressed by k/k_{NL} where k_{NL} is the cutoff of the hydrodynamic theory or fluid approximation (see e.g. [24]) and we can safely neglect here as long as we are interested in the mildly (as opposed to fully) non-linear regime. The terms in Eq. (40) are indeed those appearing in the well-known F_2 kernel. We can further massage these terms by applying to the case at hand. We take one perturbation to be long and one short, dropping terms suppressed by k_L/k_S . We are then left with only three terms:

$$\partial_i \partial_j \Phi_L \partial_i \partial_j \Phi_S, \quad \partial^2 \Phi_L \partial^2 \Phi_S, \quad \text{and} \quad \partial_i \Phi_L \partial_i \partial^2 \Phi_S. \quad (41)$$

The presence of $\partial_i \Phi_L$ in an observable quantity like δ_2 tells us immediately that this expression is valid in some set of global coordinates that are *not* free falling. In order to derive the second order effects that a local free falling observer would measure, we expand $\partial_i \Phi_L$ around the observer's geodesic

$$\partial_i \Phi_L(\mathbf{x}) = \partial_i \Phi_L(\mathbf{0}) + \partial_i \partial_j \Phi_L(\mathbf{0}) x^j + \dots \quad (42)$$

The first term in this expression, once contracted with $\partial_i \partial^2 \Phi_S$, represents the effect of the bulk flow since it can be thought of as arising from expanding $\partial^2 \Phi_S(x + U_L t)$ at linear order in u_L and using $u_L^i \sim \partial^i \Phi_L / \mathcal{H}$. This effect is present in global coordinates [as used in standard perturbation theory, see Eq. (49) below] but can be removed by a boost into the free falling local frame where $\partial_i \Phi$ vanishes.

Now that we have built some intuition, let us move to the detailed derivation. Using Eq. (6) and the fact that in global Newtonian coordinates

$$h_{00} = -2\Phi_L, \quad h_{ij} = -2\Phi_L \delta_{ij}, \quad (43)$$

we find

$$t_{ij} = -[\Phi_{L,ij} + \delta_{ij}(\mathcal{H}\Phi'_L + \Phi''_L)] \simeq -\Phi_{L,ij}, \quad (44)$$

since Φ is constant during matter domination. The transfer function [Eq. (10)] is then $T(k_L, \tau) = \text{const}$ and we can choose for simplicity $T(\tau, k_L) = 1$. Then one finds

$$F(\tau) = \frac{2}{3} H_0^{-2} a(\tau) \\ V(\tau) = D_{\sigma 2}(\tau) = \frac{4}{21} H_0^{-2} a(\tau). \quad (45)$$

Further, evaluating the Poisson equation at τ_0 where $a(\tau_0) = 1$, we have

$$t_{ij}^{(0)} = \frac{3}{2} H_0^2 \frac{\partial^i \partial^j}{\nabla^2} \delta_{1,L}(\tau_0). \quad (46)$$

Eq. (38) then yields

$$\delta_{2,s}(\mathbf{x}, \tau) = \frac{4}{7} \left(\frac{\partial^i \partial^j}{\nabla^2} \delta_{1,L}(\tau) \right) \left(\frac{\partial^i \partial^j}{\nabla^2} \delta_{1,s}(\mathbf{x}, \tau) \right) \\ + \frac{10}{7} \delta_{1,L}(\tau) \delta_{1,s}(\mathbf{x}, \tau) + \left(\frac{\partial^i \partial^j}{\nabla^2} \delta_{1,L}(\tau) \right) x^i \partial^j \delta_{1,s}(\mathbf{x}, \tau). \quad (47)$$

This expression contains precisely the terms we predicted in Eq. (41) and Eq. (42), without the bulk flow [first term in Eq. (42)]. In order to compare with the standard perturbation theory result, we have to transform from the local FNC (free falling) frame to global coordinates, which corresponds to adding back in the bulk flow. We can hence replace

$$\left(\frac{\partial_i \partial_j}{\nabla^2} \delta_{1,L} \right) x^j \rightarrow \frac{\partial_i}{\nabla^2} \delta_{1,L}. \quad (48)$$

Further, note that the other permutation corresponding to this term, i.e. $(\partial_i / \nabla^2 \delta_{1,s}) \partial_i \delta_{1,L}$ is not included in our derivation since it involves the third derivative of the long-wavelength potential, i.e. it is suppressed by k_L/k_S . Finally, in our treatment we have split $\delta_1 = \delta_{1,L} + \delta_{1,s}$ so that the second order solution contains two permutations $L \leftrightarrow s$ in the quadratic source terms. Thus, if we express the result in terms of δ_1 , we need to divide Eq. (47) by two. We finally obtain

$$\delta_2(\mathbf{x}, \tau) = \frac{2}{7} \left(\frac{\partial_i \partial_j}{\nabla^2} \delta_1(\mathbf{x}, \tau) \right) \left(\frac{\partial^i \partial^j}{\nabla^2} \delta_1(\mathbf{x}, \tau) \right) \\ + \frac{5}{7} \delta_1(\mathbf{x}, \tau) \delta_1(\mathbf{x}, \tau) + \left(\frac{\partial_i}{\nabla^2} \delta_1(\mathbf{x}, \tau) \right) \partial^i \delta_1(\mathbf{x}, \tau) \quad (49)$$

This is easily seen to be identical to the standard second order scalar density perturbation, which is usually expressed in Fourier space through the F_2 kernel (e.g., [23]).

V. TENSOR AND VECTOR MODES

In this section, we describe the effect of vector and tensor metric perturbations on the growth of small-scale fluctuations. We will focus mostly on tensor modes. All models of inflation at sufficiently high energy scale predict an approximately scale-invariant background of gravitational waves, providing strong motivation to study their effects. On the other hand, it is very difficult to devise a mechanism which produces long-wavelength vector modes while satisfying all cosmological constraints e.g. from the CMB. Our formalism is not suited to treat effects of very small scale vector modes which could have

been produced in the early Universe, since we always consider scalar perturbations with wavelengths much smaller than those of the vector modes (in any case, the effect of small scale vector modes is hard to observe unless they are coupled to long-wavelength fluctuations). However, all of the following results immediately apply to vector modes should the need arise; the only modification is in the transfer function of the long-wavelength tidal field [Eqs. (51)–(52)].

A. Tidal field

Since we work to linear order in the long-wavelength perturbations, any scalar long-wavelength perturbations in $h_{\mu\nu}$ decouple and need not be considered. We thus set $h_{00} = 0$ in Eq. (6), and the long-wavelength tensor and vector modes are contained in h_{ij} .

We define a general transfer function $D_h(\tau)$ so that

$$h_{ij}(\mathbf{0}, \tau) = D_h(\tau)h_{ij}^{(0)}, \quad (50)$$

where $h_{ij}^{(0)} = h_{ij}(\mathbf{0}, \tau = 0)$ is the primordial amplitude of the metric perturbation and $D_h(\tau \rightarrow 0) = 1$. For a single Fourier mode k_L tensor perturbation during matter domination, this transfer function is given by

$$D_{h,T}(\tau) = 3 \frac{j_1(k_L \tau)}{k_L \tau}, \quad (51)$$

while the decay of vector modes produced instantaneously at a time τ_* is described by

$$D_{h,V}(\tau) = \frac{a^2(\tau_*)}{a^2(\tau)}, \quad (52)$$

and $D_{h,V}(\tau) = 0$ for $\tau < \tau_*$.

B. Second order density

Eq. (6) yields a tidal transfer function of

$$T(\tau) = -\frac{1}{2}a^{-1}(aD'_h)', \quad (53)$$

so that

$$\begin{aligned} F(\tau) &= -\frac{1}{2}[D_h(\tau) - 1] \\ V(\tau) &= -\frac{1}{2} \int_0^\tau d\tau' \frac{\tau'^5}{\tau^5} D'_h(\tau'), \end{aligned} \quad (54)$$

where we have used that $D_h(0) = 1$. Inserting this into Eq. (38), and making use of $h_i^i = 0$ yields the second order density induced by tensor or vector mode tidal fields at time τ , in terms of the linear small-scale density field

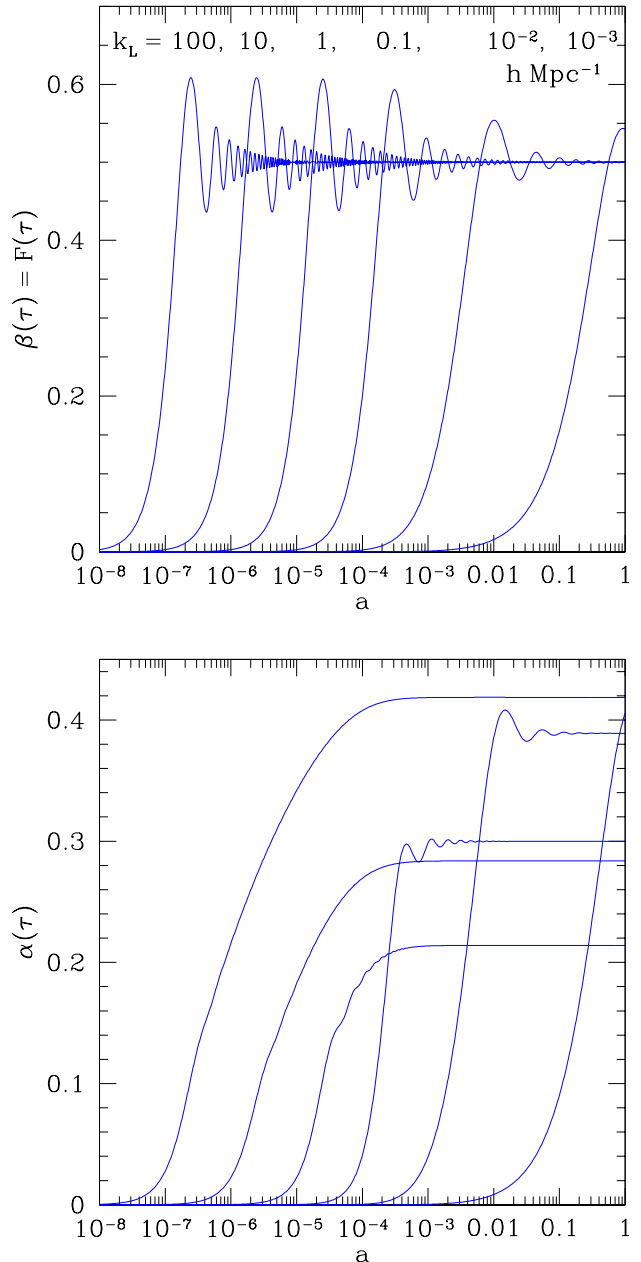


FIG. 1: *Top panel:* the function $F(\tau)$ [Eq. (54)], corresponding to $\beta(\tau)$ in Eq. (55), for tensor modes of various wavenumbers k_L as function of scale factor. *Bottom panel:* coefficient $\alpha(\tau)$ in Eq. (55), as a function of a for tensor modes with the same wavenumbers k_L as in the upper panel. For wavenumbers entering the horizon during matter domination, this reduces to Eq. (56). All results were obtained by numerical integration of the linear and second order equations (see App. C) for a flat Λ CDM cosmology.

$\delta_{1,s}$ and the *primordial* tensor mode amplitude, or vector

mode at production, respectively, $h_{ij}^{(0)}$:

$$\delta_{2,t}(\mathbf{x}, \tau) = h_{ij}^{(0)}(\mathbf{x}) \left[\alpha(\tau) \frac{\partial^i \partial^j}{\nabla^2} + \beta(\tau) x^i \partial^j \right] \delta_{1,s}(\mathbf{x}, \tau) \quad (55)$$

$$\alpha(\tau) = \frac{4}{5} \{F(\tau) - V(\tau)\} \quad (56)$$

$$= \frac{2}{5} + 18 \frac{\cos(k_L \tau)}{(k_L \tau)^4} + 6 \frac{\sin(k_L \tau)}{(k_L \tau)^3} \left[1 - \frac{3}{(k_L \tau)^2} \right],$$

$$\beta(\tau) = F(\tau) \quad (57)$$

$$= \frac{1}{2} + 3 \frac{\cos(k_L \tau)}{2(k_L \tau)^2} + 3 \frac{\sin(k_L \tau)}{2(k_L \tau)^3}.$$

This is Eq. (1) and the main analytical result of the paper. In order to elucidate its properties, we will consider tensor modes of fixed wavenumber k_L (we will briefly discuss vector modes below). In the limit of $k_L \tau \rightarrow 0$, that is before the tensor mode enters the horizon, we have

$$F(\tau) \rightarrow \frac{1}{20} (k_L \tau)^2; \quad V(\tau) \rightarrow \frac{1}{70} (k_L \tau)^2, \quad (58)$$

so that Eq. (55) becomes

$$\delta_{2,t}(\mathbf{x}, \tau) \stackrel{k_L \tau \rightarrow 0}{=} (k_L \tau)^2 h_{ij}^{(0)} \frac{1}{5} \left[\frac{1}{7} \frac{\partial^i \partial^j}{\nabla^2} + \frac{1}{4} x^i \partial^j \right] \delta_{1,s}(\mathbf{x}, \tau). \quad (59)$$

Thus, the lowest order effect of a long-wavelength tensor mode with wavenumber k_L comes in at order $(k_L \tau)^2$, as expected.

A further interesting limit to consider is $k_L \tau \gg 1$, that is long after horizon crossing of the tensor mode. In this limit, $D_h \rightarrow 0$, signifying that the tensor mode has decayed away. Thus, $V(\tau) \rightarrow 0$ while $F(\tau) \rightarrow 1/2$. Eq. (55) becomes in this ‘‘fossil’’ limit

$$\delta_{2,t}(\mathbf{x}, \tau) \stackrel{k_L \tau \rightarrow \infty}{=} h_{ij}^{(0)} \left[\frac{2}{5} \frac{\partial^i \partial^j}{\nabla^2} + \frac{1}{2} x^i \partial^j \right] \delta_{1,s}(\mathbf{x}, \tau). \quad (60)$$

The first term in Eq. (60) is the tidal interaction in the strict sense of the word. The second term corresponds to the effect of an anisotropic expansion rescaling the physical coordinates. This term has the same form as that derived by [12], the difference being that here this is just one specific limit of a more general k_L -dependent expression. One way of visualizing this term is to imagine a set of freely falling test particles in a Universe that is unperturbed apart from the tensor mode, which are initially (at $k_L \tau \ll 1$) arranged as a spherical shell $\mathbf{x}^2 = r^2$. Then, their distribution at a later time is given by

$$\mathbf{x}^2 - 2F(\tau) h_{ij}^{(0)} x^i x^j = r^2, \quad (61)$$

that is the particles have been rearranged into an ellipsoid. Note that the coefficient $F(\tau)$ of this term is valid

for a general expansion history, provided the corresponding transfer function $D_h(\tau)$ is used in Eq. (21). On the other hand, the tidal interaction term in Eq. (55) does depend on the background cosmology; for example, $V(\tau)$ depends on the behavior of the decaying scalar mode.

Finally, we point out that Eq. (55) agrees with the results of App. D in [14], which were derived for matter domination as well. Specifically, from Eq. (D19) in that paper we see that their function $2\mathcal{S}_N(K)$ is equal to α as defined in Eq. (56).

The functions $\beta(\tau) = F(\tau)$ and $\alpha(\tau)$ are shown in the upper and lower panel, respectively, of Fig. 1 as function of scale factor for various tensor mode wavenumbers k_L . As expected, $F(\tau)$ asymptotes to 1/2 long after horizon entry of the tensor mode, while $\alpha(\tau)$ asymptotes to 2/5 for modes entering the horizon during matter domination as assumed in this derivation (see curve for $k_L = 0.01 h \text{ Mpc}^{-1}$ in the lower panel of Fig. 1). We will consider the case of tensor modes entering during radiation ($k_L \gg 0.01 h \text{ Mpc}^{-1}$) and Λ domination ($k_L \ll 0.01 h \text{ Mpc}^{-1}$) in the next section.

Fig. 2 shows $\alpha(k_L, \tau)$, $\beta(k_L, \tau)$ vs k_L for two different values of the scale factor. Modes of wavenumber approaching \mathcal{H} have not decayed yet resulting in the oscillatory features around $k_L \sim 10^{-3} h \text{ Mpc}^{-1}$. The effect of modes of even longer wavelength ($k_L \ll 10^{-3} h \text{ Mpc}^{-1}$) is strongly suppressed, since they have not entered the current horizon yet. On the other hand, modes with $k_L \gg \mathcal{H}$ asymptote to a redshift-independent value, which for β is 1/2 at all wavenumbers, while for α this value is 2/5 for a narrow range of scales for which the approximation of matter domination applies.

C. Including radiation and Λ

The analytical results derived in the previous sections apply only for tensor modes which enter the horizon during matter domination. In order to extend the applicable range in k_L , we perform a numerical integration of the linear and second order equations, including radiation and a cosmological constant. The details are given in App. C. Figs. 1–2 in fact show these numerical results. Note that we have completely neglected the effects of the baryon-photon fluid before recombination. Thus, the results are only strictly valid for scalar perturbations with wavelength shorter than the dissipation scale for which the perturbations in the baryon-photon fluid are erased by viscosity.

Let us first consider the effects of radiation, important for tensor modes with $k_L \gtrsim 0.01 h \text{ Mpc}^{-1}$. On intermediate scales, there is a suppression of the second order density field, while on very small scales, we see a logarithmic increase of the effect. It is possible to qualitatively understand these trends through an analytical derivation in pure radiation domination, analogous to Sec. VB, which is described in App. D. During radiation domination, both scalar and tensor modes evolve differently than dur-

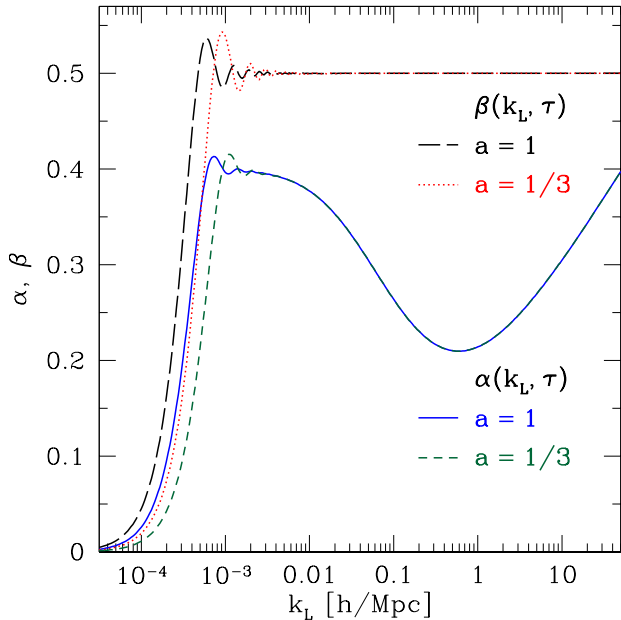


FIG. 2: Coefficient functions $\alpha(k_L, \tau)$, $\beta(k_L, \tau)$ in Eq. (55) as function of k_L for fixed scale factors $a(\tau) = 1$ and $a(\tau) = 1/3$. The same Λ CDM cosmology as in Fig. 1 was assumed.

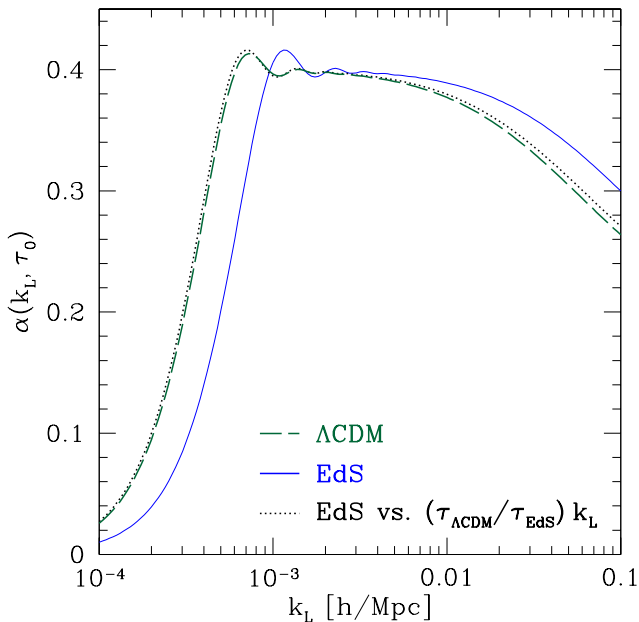


FIG. 3: Coefficient function $\alpha(k_L, \tau_0)$ as in Fig. 2 (green dashed), and for a flat matter dominated (Einstein-de Sitter, EdS) Universe (blue solid). The black dotted line shows the EdS result plotted at the same $k_L \tau$ as Λ CDM (see text). All curves are for $a(\tau_0) = 1$.

ing matter domination, with the scalar growth being proportional to $\ln \tau \propto \ln a$ rather than $a(\tau)$. The derivation of Sec. III can easily be adapted to this case (again as-

suming that the scalar perturbation is in the growing mode), leading to the result

$$\begin{aligned} \alpha_{\text{RD}}(\tau) &= V^{\text{RD}}(\tau) \\ \beta_{\text{RD}}(\tau) &= F(\tau), \end{aligned} \quad (62)$$

where the coefficient function $V^{\text{RD}}(\tau)$ is defined in Eq. (D10) while $F(\tau)$ is still given by Eq. (54) (with the appropriate D_h for radiation domination). Compared to the result for matter domination, note that the contribution to $\alpha(\tau)$, $4/5 F(\tau)$ from the second order density (fourth term in Eq. (36)) has canceled with a contribution of opposite sign in the contribution from second order evolution. This leads to the suppression on intermediate scales relative to the matter domination result. The second difference to the case of matter domination is that $V^{\text{RD}}(\tau)$ continues to evolve logarithmically even as $k_L \tau \gg 1$, explaining the trend seen for $k_L \geq 10 h \text{Mpc}^{-1}$ in Fig. 2.

We now turn to the effects of Λ . The main effect of Λ is to modify the linear scalar growth factor and the scale factor-conformal time relation. This is illustrated in Fig. 3, where we also show the result for a Universe with $\Lambda = 0$, with rescaled k_L (dotted line) so as to show results at the same value of $k_L \tau$ in both cases. We see agreement to better than 5%. Note that in the $\Lambda = 0$ case we have rescaled radiation to keep Ω_{r0}/Ω_{m0} and thus a_{eq} fixed.

In summary, while the presence of radiation and cosmological constant change the results in detail, the key result is that α remains in the range of 0.2 – 0.5 over the entire range of accessible tensor wavenumbers, and the range of redshifts relevant for large-scale structure. Thus, we do not confirm the expectation of [14] who argued that the effect should be strongly suppressed for modes $k_L \gtrsim 0.01 h \text{Mpc}^{-1}$.

VI. IMPACT ON SMALL-SCALE DENSITY STATISTICS

Consider a region of size $R \ll 1/k_L$ over which a tensor mode h_{ij} with wavenumber k_L can be considered spatially constant (as described in Sec. II, this region is entirely contained within the conformal Fermi patch corresponding to the tensor mode). Corrections will be suppressed by powers of k_L/k_S , where k_S is the wavenumber of the scalar perturbation considered. We now show how the results for the second-order density $\delta_{2,t}$ from the previous section predict a modification of the small-scale correlation function $\xi_F(\mathbf{r})$ of the matter density field measured locally, that is in the $\overline{\text{FNC}}$ frame.

We define the local two-point function in $\overline{\text{FNC}}$ $\xi_F(\mathbf{r}, \tau)$ through

$$\xi_F(\mathbf{r}, \tau) = \langle \delta_F(\mathbf{0}, \tau) \delta_F(\mathbf{r}, \tau) \rangle, \quad (63)$$

where

$$\delta_F(\mathbf{x}, \tau) = \delta_{1,s}(\mathbf{x}, \tau) + \delta_{2,t}(\mathbf{x}, \tau). \quad (64)$$

Analogously, we define the linear matter correlation function $\xi_{1,s}$, i.e. that of $\delta_{1,s}$. By assumption $r \ll 1/k_L$. Inserting Eq. (55) yields

$$\begin{aligned} \xi_F(\mathbf{r}, \tau) &= \xi_{1,s}(r, \tau) \\ &\quad + h_{ij}^{(0)} \left[2\alpha(\tau) \frac{\partial^i \partial^j}{\nabla^2} + \beta(\tau) r^i \partial_j \right] \xi_{1,s}(r, \tau) \\ &= \xi_{1,s}(r, \tau) + h_{ij}^{(0)} \hat{r}^i \hat{r}^j \left[2\alpha(\tau) \left(\xi''_{\nabla^{-2}\delta_{1,s}}(r) - \frac{1}{r} \xi'_{\nabla^{-2}\delta_{1,s}}(r) \right) \right. \\ &\quad \left. + \beta(\tau) \frac{d\xi_{1,s}(r, \tau)}{d \ln r} \right], \end{aligned} \quad (65)$$

where primes denote derivatives with respect to r and

$$\xi_{\nabla^{-2}\delta_{1,s}}(r, \tau) = - \int \frac{d^3 \mathbf{k}}{(2\pi)^3} k^{-2} P_{1,s}(k, \tau) e^{i\mathbf{k}\mathbf{r}}. \quad (66)$$

Note that the same result is obtained when defining Eq. (63) as $\langle \delta_F(-\mathbf{r}/2) \delta_F(\mathbf{r}/2) \rangle$. We can Fourier transform Eq. (65) to obtain the local power spectrum. This parallels the calculation in App. B of [15] and yields

$$\begin{aligned} P_\delta(\mathbf{k}, \tau|h) - P_\delta(k, \tau) &= \hat{k}^i \hat{k}^j h_{ij}^{(0)} P_\delta(k, \tau) \\ &\quad \times \left[2\alpha(\tau) - \beta(\tau) \frac{d \ln P_\delta(k, \tau)}{d \ln k} \right]. \end{aligned}$$

This is Eq. (2).

Eq. (65) applies to the matter density field. In reality, one observes the statistics of some tracer of matter which is generally biased, i.e. whose clustering properties are not identical to those of matter. The simplest case is a linear local bias. Then, Eq. (65) remains valid for the tracers if $\xi_{1,s}$ is replaced with

$$\xi_{1,s,g}(r) = b_1^2 \xi_{1,s}(r), \quad (67)$$

where b_1 is the linear bias. Two conditions need to be fulfilled for this to be valid: first, the matter correlation $\xi_{1,s}(r)$ on the scale r has to be small, so that corrections of order $[b_2 \xi_{1,s}(r)]^2$ are negligible, where b_2 is the quadratic bias of the tracer. Second, any non-locality in the relation between tracer number density and matter density has to be restricted to scales much smaller than r . These two conditions are likely to be satisfied by the 21cm emission from the dark ages which was considered in [12, 16]. On the other hand, for galaxy surveys at lower redshifts, these conditions are not met in general, necessitating a higher order perturbative treatment, which we will not attempt here.

A. Projection effects

Eq. (65) gives the effect of tensor modes on small-scale correlations that would be observed locally by a comoving observer, i.e. in the observer's $\overline{\text{FNC}}$ frame. In the end however, we want to know the effect on the small-scale

correlations as observed from Earth, specifically through the arrival directions and redshifts of photons. We thus need to add the effects of the mapping from $\overline{\text{FNC}}$ (source location) to $\overline{\text{FNC}}$ (Earth), which we refer to as ‘‘projection effects’’.³ Note that since the two frames are uniquely defined (at the relevant order), these projection effects are gauge-invariant. As described in Sec. IV of [15], there are three ingredients to this mapping:

- The transformation of the correlation scale \mathbf{r} through the cosmic ruler perturbations derived in [1].
- A shift in time from fixed proper time at $\overline{\text{FNC}}$ (source) to fixed observed redshift on Earth, as derived in [25].
- A modulation of the mean observed density within the patch over which the small-scale correlation is measured. The modulation of the observed density of a general tracer by tensor modes was derived in [26].

As shown in App. E, it is straightforward to collect all these results to obtain

$$\begin{aligned} \xi(\mathbf{r}, \tau|h) &= \left[1 + \left\{ \frac{1}{2} \int_0^{\bar{\chi}} d\chi h'_{\parallel} \delta_{ij} + \frac{1}{2} h_{ij} + \partial_{(i} \Delta x_{j)} \right\} r^i \partial_r^j \right. \\ &\quad \left. + \frac{1}{2\mathcal{H}} \int_0^{\bar{\chi}} d\chi h'_{\parallel} \partial_\tau \right. \\ &\quad \left. + 2 \left\{ \frac{b_e}{2} \int_0^{\bar{\chi}} d\chi h'_{\parallel} + \partial_i \Delta x^i + \mathcal{Q} \mathcal{M}_T \right\} \right] \xi_F(\mathbf{r}; \tau), \end{aligned} \quad (68)$$

where again $\xi_F(\mathbf{r}, \tau)$ is the small-scale correlation function in the $\overline{\text{FNC}}$ frame. Here, metric perturbations outside integrals are evaluated at the source, while metric perturbations inside integrals are evaluated on the past lightcone in the background (see App. E for details). Further, $h_{\parallel} \equiv h_{ij} \hat{n}^i \hat{n}^j$, $\hat{\mathbf{n}}$ is the unit vector along the line of sight, and $\bar{\chi} \equiv \bar{\chi}(\bar{z})$ where $\bar{\chi}(z)$ is the comoving distance-redshift relation in the background and \bar{z} is the observed redshift. Δx^i , defined in Eqs. (E4)–(E5) denote the displacement of the true source position from the apparent position. \mathcal{M}_T is the gauge-invariant magnification produced by the tensor mode and is given in Eq. (E14). Further, there are two tracer-dependent parameters: the magnification bias parameter \mathcal{Q} , given in the simplest case of a sharp flux-limited survey by $\mathcal{Q} = -d \ln \bar{n}_g / d \ln f_{\text{cut}}$; and the parameter b_e , which quantifies the redshift evolution of the comoving number density of tracers through Eq. (E17).

³ As long as the region over which we measure small-scale correlations is much smaller than the horizon, which is always the case in practice, the distinction between FNC and $\overline{\text{FNC}}$ is irrelevant (Sec. II).

We now insert Eq. (65) for ξ_F in Eq. (68), which effectively results in adding up all tensor mode effects. We then obtain

$$\begin{aligned} \xi(\mathbf{r}, \tau|h) = & \left[1 + \left\{ \frac{1}{2} \int_0^{\bar{\chi}} d\chi h'_{\parallel} \delta_{ij} + \frac{1}{2} h_{ij} + \partial_{(i} \Delta x_{j)} \right\} r^i \partial_r^j \right. \\ & + \frac{1}{2\mathcal{H}} \int_0^{\bar{\chi}} d\chi h'_{\parallel} \partial_\tau \\ & + 2 \left\{ \frac{b_e}{2} \int_0^{\bar{\chi}} d\chi h'_{\parallel} + \partial_i \Delta x^i + \mathcal{Q} \mathcal{M}_T \right\} \\ & \left. + 2h_{ij}^{(0)} \left\{ \alpha(\tau) \frac{\partial^i \partial^j}{\nabla^2} + \beta(\tau) r^i \partial_j \right\} \right] \xi_{1,s}(r; \tau). \end{aligned} \quad (69)$$

For biased tracers, we again just need to replace $\xi_{1,s}$ with $b_1^2 \xi_{1,s}$ as long as linear local bias is sufficient. This result agrees with [14], with the exception of the magnification bias contribution $\mathcal{Q}\mathcal{M}_T$ which they did not include.

VII. SHEAR CORRELATION AND INTRINSIC ALIGNMENTS

We now turn to the signature of tensor modes in galaxy shear surveys. As discussed in [13, 27], the effect of tensor modes on photon geodesics leads to a contribution to the weak lensing shear which can be measured through the correlations of galaxy shapes (second moments). Specifically, a gravitational wave background contributes to the parity-odd B-mode component, which does not receive any scalar contribution at linear order and thus provides a window to search for gravitational waves.

The tensor-mode contribution to the shear, which is a tracefree symmetric tensor on the sky (with two independent components) is given by [13]

$$\gamma_{ij}^{\text{proj}} = -\frac{1}{2} \mathcal{P}_i^k \mathcal{P}_j^l h_{kl} - \partial_{\perp(i} \Delta x_{\perp j)}, \quad (70)$$

where $\mathcal{P}_{kl} = \delta_{kl} - \hat{n}_k \hat{n}_l$ is the projection operator onto the sky plane, $\partial_{\perp i} = \mathcal{P}_i^j \partial_j$, and the displacement Δx_{\perp} is given in Eq. (E5).

Eq. (70) gives the contribution to galaxy shape correlations induced by the mapping from the source's $\overline{\text{FNC}}$ frame to observed coordinates, in analogy with the projection effects discussed in Sec. VIA [in fact, γ_{ij} is part of the terms appearing in the first line of Eq. (68)]. However, we expect that the effect of tensor modes on the local density field described by $\delta_{2,t}$ [Eq. (55)] also affects galaxy shapes; that is, there is also a correlation of galaxy shapes with the local tidal field in the $\overline{\text{FNC}}$ frame, leading to a contribution to shape correlations which we will denote as γ_{ij}^{IA} . In the terminology of weak lensing shear, this effect is referred to as *intrinsic alignment*. Just as in Sec. VIA, the *observed* correlation of galaxy shapes is then given by the sum of the two contributions,

$$\gamma_{ij}^{\text{obs}} = \gamma_{ij}^{\text{proj}} + \gamma_{ij}^{\text{IA}}. \quad (71)$$

We now consider the intrinsic alignment contribution in more detail. It is difficult to predict the amplitude of the alignment of galaxy shapes with the large-scale tidal field from first principles. For tensor modes, this effect was first considered by Schmidt and Jeong [13], who used observations of alignments with scalar tidal fields to estimate the effect for gravitational waves. Using our results from Sec. V, we can elaborate a bit more on this effect. We have found above that the second order density field induced by the (trace-free component of) a *scalar* tidal field is given by

$$\delta_{2,s} = \frac{2}{7} \left(\frac{\partial_i \partial_j}{\nabla^2} \delta_{1,L}(\mathbf{x}, \tau) \right) \frac{\partial^i \partial^j}{\nabla^2} \delta_{1,s}(\mathbf{x}, \tau), \quad (72)$$

while that of a tensor mode is given by

$$\delta_{2,t} = \alpha(k_L, \tau) h_{ij}^{(0)} \frac{\partial^i \partial^j}{\nabla^2} \delta_{1,s}(\mathbf{x}, \tau). \quad (73)$$

One possible way to estimate the intrinsic alignment by tensor modes is to assume that the alignment scales as the second order density perturbation induced by the external tidal field. The alignment by scalar tidal fields has observationally been measured at low redshift for elliptical galaxies [28–30]. The scalar intrinsic alignment contribution to the shear can be parametrized as

$$\gamma_{ij}^{\text{IA},s}(\mathbf{x}, \tau) = -\Omega_{m0} \tilde{C} a^{-1}(\tau_P) \mathcal{P}_i^k \mathcal{P}_j^l \left(\frac{\partial_k \partial_l}{\nabla^2} \delta(\mathbf{x}, \tau_P) \right),$$

where τ is the observation epoch while τ_P is the epoch at which the tidal field is evaluated. Note that since scalar tidal fields do not evolve strongly, the precise value of τ_P does not change results by more than 30%. In the following, we will choose $\tau_P = \tau$. For the $z = 0.2 - 0.4$ luminous red galaxies (LRG) studied in [29, 30], $\tilde{C} = C_{1\rho_{\text{cr},0}} \approx 0.12$. Thus, by matching the second order density induced by scalar and tensor tidal fields at the observation epoch, we arrive at the following estimate for the tensor contribution to intrinsic alignments:

$$\gamma_{ij}^{\text{IA},t}(\mathbf{x}, \tau) = -\Omega_{m0} \tilde{C} \frac{7}{2} \frac{\alpha(k_L, \tau)}{a(\tau)} \mathcal{P}_i^k \mathcal{P}_j^l h_{kl}^{(0)}(\mathbf{x}). \quad (74)$$

Fig. 4 shows the resulting predicted angular power spectrum of the B-mode of the shear, assuming an almost scale-invariant gravitational wave background with tensor-to-scalar ratio $r = 0.1$ (that is, exactly one half of the value adopted in [13], with otherwise identical parameters). The solid lines show the result obtained using the matching relation Eq. (74) at observed redshift $z = 0.8$ (thin) and $z = 2$ (thick), respectively. Here, we have used the numerical results for ΛCDM (App. C) for the coefficient $\alpha(k_L, \tau)$, as shown in Fig. 2. The dotted lines in Fig. 4 show the result for $\tilde{C} = 0$, i.e. when only the lensing (projection) effect contributes and any alignment effect of the tensor mode tidal field is absent. Clearly, the lensing effect is at least one order of magnitude smaller than the estimated alignment effect,

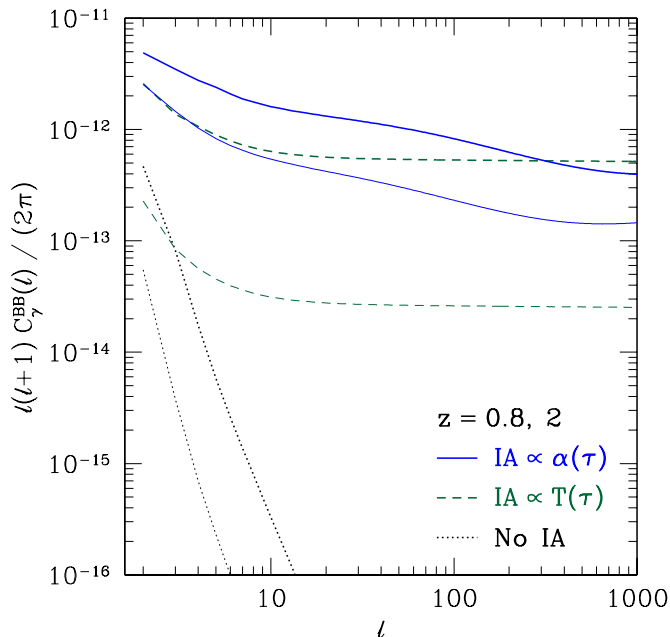


FIG. 4: Tensor mode contribution to the B mode angular shear power spectrum from a gravitational wave background with tensor-to-scalar ratio $r = 0.1$. The blue solid lines show the result using the matching of the second order density [Eq. (74)], green dashed lines show the result when using the instantaneous tensor tidal field as adopted in [13], and black dotted lines show the result in the absence of intrinsic alignment, i.e. only including the lensing contribution. In all cases, thick lines are for a source redshift of $z = 2$, while thin lines are for $z = 0.8$.

and moreover drops much more rapidly towards higher ℓ (smaller scales).

The long-dashed lines in Fig. 4 show the previous prescription adopted in [13], which relates the shear to the instantaneous tidal field induced by tensor modes,

$$\gamma_{ij}^{\text{IA,t}}(\mathbf{x}, \tau) = \tilde{C} \mathcal{P}_i^k \mathcal{P}_j^l t_{kl}^{\text{tensor}}(\mathbf{x}, \tau), \quad (75)$$

for the same redshifts. Unlike Eq. (74), this relation only yields a contribution to the shear for tensor modes that have recently entered the horizon. For a relatively high source redshift of $z = 2$, the prediction from the second order density-matching is a factor of 2 – 4 larger than the prediction using Eq. (75) on large scales, well within the uncertainty of these rough estimates, while at lower source redshifts the difference becomes much larger (factor of ~ 30 at $z = 0.8$). This is because the effect has more time to build up in Eq. (74), i.e. a wider range in wavenumber contributes to the alignment signal. Consequently, in this ansatz the redshift-dependence of the alignment contribution is significantly weaker (it is almost entirely due to the $a^{-1}(\tau)$ prefactor in Eq. (74), given the redshift independence of the tidal imprint on the second order density field for $k_L \gg \mathcal{H}$). The redshift dependence is weaker at the lowest ℓ , because very

large scale tensor modes that have recently entered the horizon have had less time to build up an effect at earlier times. Finally, we point out that the redshift dependence of the alignment strength of galaxies is very uncertain at this point and likely depends strongly on the particular galaxy sample considered.

Nevertheless, the fact that the signal is much larger at low source redshifts than what was estimated in [13] greatly improves the observational prospects for detecting this effect. Note also the slow suppression of the signal for $\ell \gtrsim 100$ of the alignment signal predicted by Eq. (74), which is due to the suppression of the second order density in the range $0.01 < k_L [h/\text{Mpc}] < 1$ [Fig. 2]; however, given the order-of-magnitude uncertainty of this estimate such details of the predicted signal should be taken with a grain of salt.

Finally, in our prediction of γ_{ij}^{IA} , we have only considered the first term in Eq. (49) and Eq. (55), respectively. There might also be a contribution from the differential displacement [second term in Eq. (55) and last two terms in Eq. (49)] to the orientation of galaxies in both scalar and tensor cases, but investigating the relative contribution of this term goes beyond the scope of this paper.

VIII. CONCLUSIONS

In this paper we have computed the effect of long-wavelength perturbations on the dynamics of short-wavelength matter inhomogeneities. We made crucial use of conformal Fermi Normal Coordinates (FNC) in order to isolate the physical effects and remove unobservable coordinate artifacts. This ensures that the results of the various steps of our computations are individually observable. Our formalism can be applied to scalar, vector and tensor long-wavelength perturbations. The case of scalars is well-known and provides a nice check of our results. For vector and tensor perturbations we find that the effect on the short-wavelength matter inhomogeneity is given by Eq. (1), with the consequent anisotropy in the power spectrum given by Eq. (2). Interestingly, these effects remain of order $h_{ij}^{(0)}$ in the $k_L \tau \gg 1$ (fossil) limit, even for wavenumbers k_L which have entered the horizon during radiation domination.

All these results are given in the reference frame of a comoving observer. We have also computed projection effects necessary to make contact with what is observed from Earth. The projected 2-point function of matter (or linearly biased tracers) is given in Eq. (69) as an example, but other projected quantities can be straightforwardly computed as well. Although we have not done so, this can also be easily coupled to the signal-to-noise forecasts for 21cm correlations performed in [16, 31]. Further, it would be interesting to study other large-scale structure tracers as probes of this effect, and cross-correlations between them and the cosmic microwave background.

A further important pertinent observable is cosmic shear, i.e. correlations of galaxy shapes. Here, the lo-

cally observable (“tidal”) effects and projection effects are commonly known as “intrinsic alignments” and “lensing”, respectively. We have made the rough approximation that the tidal alignment of galaxies scales as the anisotropic contribution to the second order density field. The resulting odd parity B-mode power spectrum, to which there are no scalar contributions at linear order, is shown in Fig. 4. Interestingly, the tidal effects are much stronger than the lensing effects for tensor modes, while the converse is true for standard scalar density perturbations. Moreover, we have found that the residual effect in the density field which remains when $k_T\tau \gg 1$ [Eq. (60)] greatly enhances the expected signal for source galaxies at low redshifts ($z < 2$).

The assumption that galaxy alignments scale with the anisotropic part of the second order density field can only be seen as a rough approximation. It would thus be interesting to perform N-body simulations with an external tidal field imposed, which mimics the effect of a long-wavelength gravitational wave. One could then study the alignment of dark matter halos and substructure with this external tidal field.

Another approximation we have made throughout is to neglect the effects of the baryon-photon fluid before

recombination. This issue can be studied using the same tools as presented here. However, since the fluid is relativistic, one also has to take into account the metric components g_{0i}^F and g_{ij}^F . We leave this for future work as well.

Acknowledgments

We are happy to thank L. Dai, D. Jeong and M. Kamionkowski for helpful discussions. We further thank K. Masui for discussions and pointing out a factor of 2 mistake in Sec. VI. E. P. was supported in part by the Department of Energy grant DE-FG02-91ER-40671. F. S. acknowledges support at Princeton by NASA through Einstein Postdoctoral Fellowship grant number PF2-130100 awarded by the Chandra X-ray Center, which is operated by the Smithsonian Astrophysical Observatory for NASA under contract NAS8-03060. M. Z. is supported in part by the National Science Foundation grants PHY-0855425, AST-0907969, PHY-1213563 and by the David & Lucile Packard Foundation.

Appendix A: Derivation of Eqs. (5)–(6)

This section deals with the transformation of the metric from a set of global coordinates Eq. (3) to $\overline{\text{FNC}}$, specifically the time-time component. We will set $h_{0i} = 0$ and only keep h_{00} and h_{ij} , since this is sufficient to treat scalar perturbations in all widespread gauge choices as well as tensor perturbations. The relation between global coordinates and $\overline{\text{FNC}}$ is then [15]

$$x^0(\bar{x}_F^\alpha) = \bar{x}_F^0 + \frac{1}{2} \int_0^{\bar{x}_F^0} h_{00}(\tau) d\tau + u_i \bar{x}_F^i - \frac{1}{4} h'_{ij} \bar{x}_F^i \bar{x}_F^j + \mathcal{O}[(\bar{x}_F^i)^3] \quad (\text{A1})$$

$$x^k(\bar{x}_F^\alpha) = u^k(\bar{x}_F^0 - \tau_F) + \bar{x}_F^k - \frac{1}{2} h^k_{iF} \bar{x}_F^i - \frac{1}{4} [h^k_{i,j} + h^k_{j,i} - h_{ij}{}^{,k}] \bar{x}_F^i \bar{x}_F^j + \mathcal{O}[(\bar{x}_F^i)^3], \quad (\text{A2})$$

where u^i is the coordinate velocity of the central geodesic, and all perturbations are evaluated at the central geodesic, i.e. at $\bar{\mathbf{x}}_F = 0$. First, let us verify that using this coordinate transform, the conformal metric $\eta_{\mu\nu} + h_{\mu\nu}$ becomes $\eta_{\mu\nu} + \mathcal{O}[(\bar{x}_F^i)^2]$, i.e. Eq. (14) in [15]. We have

$$\begin{aligned} \frac{\partial x^0}{\partial \bar{x}_F^0} &= 1 + \frac{1}{2} h_{00}(\mathbf{0}, \bar{x}_F^0) + u'_i \bar{x}_F^i \\ \frac{\partial x^i}{\partial \bar{x}_F^0} &= u^i. \end{aligned} \quad (\text{A3})$$

Neglecting terms of order $(u/c)^2$, the central point has a four-velocity

$$v^\mu = \frac{dP^\mu}{dx^0} = \left(1 + \frac{1}{2} h_{00}, u^i \right) \quad (\text{A4})$$

which follows the geodesic equation for the metric $\eta_{\mu\nu} + h_{\mu\nu}$ whose spatial components are

$$u^i = -\Gamma_{00}^i (1 + \mathcal{O}(h))^2 = \frac{1}{2} \partial^i h_{00}. \quad (\text{A5})$$

We are interested in the time-time component of the conformal metric, which we denote \bar{g}_{00} . In global coordinates, it is given by

$$\bar{g}_{00}(x) = \eta_{00} + h_{00}(x) = -1 + h_{00}(\mathbf{0}, \tau) + \partial_i h_{00}(\mathbf{0}, \tau) x^i + \frac{1}{2} \partial_i \partial_j h_{00}(\mathbf{0}, \tau) x^i x^j + \mathcal{O}[(x^i)^3], \quad (\text{A6})$$

where we have chosen the global coordinate origin to coincide with that of the $\overline{\text{FNC}}$ frame at the specific time considered. In going to $\overline{\text{FNC}}$, the second term is immediately canceled by the second term in Eq. (A1), while the third, gradient term is canceled by the u^i term in Eq. (A1) together with the geodesic equation. Thus, we obtain for the 00 component of the conformal metric in $\overline{\text{FNC}}$ coordinates

$$\bar{g}_{00}^F = \eta_{00} + \frac{1}{2} \partial_i \partial_j h_{00} \bar{x}_F^i \bar{x}_F^j + \frac{1}{2} h''_{ij} \bar{x}_F^i \bar{x}_F^j, \quad (\text{A7})$$

where again h is evaluated at $\mathbf{0}$. Here, we have replaced $x^i \rightarrow \bar{x}_F^i$ at this order. This is Eq. (14) of [15].

We now consider physical metric, that is $g_{\mu\nu} = a^2(\tau)[\eta_{\mu\nu} + h_{\mu\nu}]$. First, the origin of the $\overline{\text{FNC}}$ frame is now constrained to follow a geodesic in the physical metric. The four-velocity is given by (e.g., [1])

$$v^\mu = \frac{dx^\mu}{d\lambda} = a^{-1}(x^0) \left(1 + \frac{1}{2} h_{00}(x), u^i(x) \right). \quad (\text{A8})$$

The relevant Christoffel components are

$$\begin{aligned} \Gamma_{00}^i &= \frac{1}{2} a^{-2} \left[-a^2 h_{00}{}^{,i} \right] = -\frac{1}{2} \partial^i h_{00} \\ \Gamma_{0j}^i &= \frac{1}{2} a^{-2} \left[g^i{}_{j,0} \right] = \frac{a'}{a} \delta^i{}_j + \mathcal{O}(h) = \mathcal{H} \delta^i{}_j + \mathcal{O}(h). \end{aligned} \quad (\text{A9})$$

Since Γ_{0j}^i multiplies u , we do not have to include the h terms there. We then obtain for the i -component of v^μ

$$\begin{aligned} \frac{d}{d\lambda} \left(\frac{u^i}{a} \right) &= (v^0) \left(\frac{u^i}{a} \right)' = -\Gamma_{00}^i (v^0)^2 - 2\Gamma_{0j}^i v^0 v^j = a^{-2} \left[\frac{1}{2} \partial^i h_{00} - 2\mathcal{H} u^i \right] \\ \Rightarrow u'^i &= \frac{1}{2} \partial^i h_{00} - \mathcal{H} u^i. \end{aligned} \quad (\text{A10})$$

Note that this agrees with the Euler equation in Eq. (B3) once linearized. Eq. (A3) is still valid, since u^i in Eq. (A3) is defined as dP^i/dx^0 and

$$\frac{dP^i}{dx^0} = \frac{dx^i/d\lambda}{dx^0/d\lambda} = \frac{v^i}{v^0} = u^i, \quad (\text{A11})$$

recalling that u^i is first order. We now transform g_{00} to g_{00}^F in $\overline{\text{FNC}}$. Using Eq. (A10), we obtain

$$g_{00}^F = a^2 (x^0[\bar{x}_F]) \left[-1 + 2\mathcal{H} u_i \bar{x}_F^i + \frac{1}{2} \partial_i \partial_j h_{00} \bar{x}_F^i \bar{x}_F^j + \frac{1}{2} h''_{ij} \bar{x}_F^i \bar{x}_F^j \right]. \quad (\text{A12})$$

We expand the prefactor $a^2(x^0[\bar{x}_F])$ as follows:

$$a^2(x^0[\bar{x}_F]) = a^2 \left(\bar{x}_F^0 + \frac{1}{2} \int h_{00} d\tau \right) \left[1 + 2\mathcal{H} u_i \bar{x}_F^i - \frac{1}{2} \mathcal{H} h'_{ij} \bar{x}_F^i \bar{x}_F^j \right]. \quad (\text{A13})$$

Putting everything together, the 00 component of the physical metric in $\overline{\text{FNC}}$ becomes

$$g_{00}^F = a_F^2(\bar{x}_F^0) \left[-1 + \frac{1}{2} \partial_i \partial_j h_{00} \bar{x}_F^i \bar{x}_F^j + \frac{1}{2} h''_{ij} \bar{x}_F^i \bar{x}_F^j + \frac{1}{2} \mathcal{H} h'_{ij} \bar{x}_F^i \bar{x}_F^j \right] \quad (\text{A14})$$

$$a_F(\bar{x}_F^0) \equiv a \left(\bar{x}_F^0 + \frac{1}{2} \int h_{00}(\mathbf{0}, \tau) d\tau \right). \quad (\text{A15})$$

This corresponds to Eqs. (5)–(6). g_{00}^F is, apart from the scale factor, clearly in the FNC form, with corrections going as spatial distance from the central geodesic squared. The fact that the scale factor is evaluated at $\bar{x}_F^0 + \frac{1}{2} \int h_{00}(\mathbf{0}, \tau) d\tau$

might surprise at first. Note however that by construction, at $\bar{\mathbf{x}}_F = 0$ the coordinate \bar{x}_F^0 is the proper time along the central geodesic with respect to the metric $\eta_{\mu\nu} + h_{\mu\nu}$, so that

$$t_F \equiv \int^{\bar{x}_F^0} a [x^0(\tau, \bar{\mathbf{x}}_F = 0)] d\tau = \int^{\bar{x}_F^0} a_F(\tau) d\tau \quad (\text{A16})$$

is the proper time (with respect to the physical metric $g_{\mu\nu}$) along the central geodesic. Thus, evaluating Eq. (A14) at $\bar{\mathbf{x}}_F = 0$ yields

$$dt_F = a_F(\bar{x}_F^0) d\bar{x}_F^0. \quad (\text{A17})$$

In other words, \bar{x}_F^0 has a clear interpretation as ‘‘conformal proper time’’. In particular for $h_{00} = 0$, $t_F = t$, where t is the time coordinate, and $\bar{x}_F^0 = \tau$, where τ is the corresponding conformal time. For $h_{00} \neq 0$, the non-trivial argument of the scale factor in Eq. (A15) expresses the fact that constant-proper-time surfaces are *not* constant-scale-factor surfaces. If we transform to the standard FNC frame, i.e. to physical rather than comoving coordinates, we obtain metric corrections of the form $H^2 \mathbf{x}_F^2$, $\dot{H} \mathbf{x}_F^2$, where H is the Hubble rate evaluated at the time coordinate corresponding to the given proper time along the central geodesic, i.e. at $\bar{x}_F^0 + \frac{1}{2} \int h_{00}(\mathbf{0}, \tau) d\tau$ just as in the scale factor above. The apparent unphysical dependence on a metric perturbation h_{00} (without any derivative) is simply because we are referring to an unobservable ‘‘background’’ scale factor here. A local observer moving along the central geodesic will simply measure the Hubble rate as a function of his/her proper time (this is in fact is how we define our background scale factor in practice). Thus, the scale factor multiplying the metric Eq. (A14) is the scale factor that would *locally be reconstructed* from the measured Hubble rate, hence our notation of $a_F(\bar{x}_F^0)$ in Eq. (5).

Appendix B: Eulerian derivation

In this section we present an independent derivation of the main results of Sec. III using Eulerian perturbation theory. We define the peculiar velocity through

$$\mathbf{u} = \frac{d\mathbf{x}}{d\tau} = a(t) \frac{d\mathbf{x}}{dt} = a\mathbf{v} - \mathcal{H}\mathbf{x}, \quad \mathbf{v} = \frac{d\mathbf{r}}{dt}. \quad (\text{B1})$$

The continuity and Euler equations for an ideal fluid are then given by

$$\delta' + \nabla \cdot [(1 + \delta)\mathbf{u}] = 0 \quad (\text{B2})$$

$$\mathbf{u}' + (\mathbf{u} \cdot \nabla)\mathbf{u} + \mathcal{H}\mathbf{u} = -\nabla\Phi - \frac{1}{\rho}\nabla(\rho\sigma), \quad (\text{B3})$$

where σ_{ij} is the stress tensor of the fluid including pressure (here, $[\nabla(\rho\sigma)]^i = \partial_j(\rho\sigma^{ij})$). In the following, we will set $\sigma_{ij} = 0$. Separating density and velocity into parts zeroth and first order in t_{ij} , we write

$$\delta = \delta_s + \delta_t; \quad \mathbf{u} = \mathbf{u}_s + \mathbf{u}_t, \quad (\text{B4})$$

where δ_s , \mathbf{u}_s ; δ_t , \mathbf{u}_t satisfy

$$\begin{aligned} \delta'_s + \nabla \cdot [(1 + \delta_s)\mathbf{u}_s] &= 0 \\ \mathbf{u}'_s + (\mathbf{u}_s \cdot \nabla)\mathbf{u}_s + \mathcal{H}\mathbf{u}_s &= -\nabla\Phi_s \end{aligned} \quad (\text{B5})$$

$$\begin{aligned} \delta'_t + \nabla \cdot \mathbf{u}_t + \nabla \cdot [\delta_s \mathbf{u}_t + \delta_t \mathbf{u}_s] &= 0 \\ [\mathbf{u}'_t + (\mathbf{u}_s \cdot \nabla)\mathbf{u}_t + (\mathbf{u}_t \cdot \nabla)\mathbf{u}_s + \mathcal{H}\mathbf{u}_t]^i &= -T(\tau) t^{(0)i}_j x^j. \end{aligned} \quad (\text{B6})$$

The linearized equations are easily seen to be equivalent to the corresponding Lagrangian equations. Hence, we can make use of Eqs. (18)–(23) for the linear solutions. In particular,

$$\begin{aligned} u^i_{1,s}(\mathbf{x}, \tau) &= -a'(\tau) \frac{\partial^i}{\nabla^2} \delta_{1,s}(\mathbf{x}, \tau_0) \\ u^i_{1,t}(\mathbf{x}, \tau) &= -F'(\tau) t^{(0)i}_j x^j \\ \delta_{1,t}(\mathbf{x}, \tau) &= F(\tau) t^{(0)i}_i. \end{aligned} \quad (\text{B7})$$

1. Second order solution

As in the Lagrangian derivation (Sec. III), we work in a perturbative expansion in all of δ_s , \mathbf{u}_s ; δ_t , \mathbf{u}_t , i.e.

$$\mathbf{u}_t = \mathbf{u}_{1,t} + \mathbf{u}_{2,t} + \dots, \quad (\text{B8})$$

and derive the leading corrections $\delta_{2,t}$, $\mathbf{u}_{2,t}$. These corrections obey the equations

$$\delta'_{2,t} + \nabla \cdot \mathbf{u}_{2,t} = -\nabla \cdot [\delta_{1,s} \mathbf{u}_{1,t} + \delta_{1,t} \mathbf{u}_{1,s}] \quad (\text{B9})$$

$$\mathbf{u}'_{2,t} + (\mathbf{u}_{1,s} \cdot \nabla) \mathbf{u}_{1,t} + (\mathbf{u}_{1,t} \cdot \nabla) \mathbf{u}_{1,s} + \mathcal{H} \mathbf{u}_{2,t} = -\nabla \Phi_s^{(2)}. \quad (\text{B10})$$

Taking the divergence of the second equation, assuming Einstein-de Sitter, and introducing $\theta_{2,t} = \nabla \cdot \mathbf{u}_{2,t}$ allows us to write these equations as

$$\begin{aligned} \delta'_{2,t} + \theta_{2,t} &= -S_1 \\ \theta'_{2,t} + \mathcal{H} \theta_{2,t} + \frac{3}{2} \mathcal{H}^2 \delta_{2,t} &= -S_2 \\ S_1 &= -\left[a F' t_{ij}^{(0)} x^i \partial^j + (aF)' t_i^{(0)j} \right] \delta_{1,s}^{(0)} \\ S_2 &= \nabla \cdot [(\mathbf{u}_{1,s} \cdot \nabla) \mathbf{u}_{1,t} + (\mathbf{u}_{1,t} \cdot \nabla) \mathbf{u}_{1,s}] \\ &= a' F' t_{ij}^{(0)} \left[2 \frac{\partial^i \partial^j}{\nabla^2} \delta_{1,s}^{(0)} + x^i \partial^j \delta_{1,s}^{(0)} \right]. \end{aligned} \quad (\text{B11})$$

Here, $\delta_{1,s}^{(0)}$ stands for the linear scalar density at a reference time τ_0 , i.e. with the growth taken out. We now take the derivative with respect to τ of the continuity equation and insert the Euler equation for $\theta'_{2,t}$. This yields

$$\delta''_{2,t} + \mathcal{H} \delta'_{2,t} - \frac{3}{2} \mathcal{H}^2 \delta_{2,t} = -[S'_1 + \mathcal{H} S_1] + S_{2,t} = -\frac{1}{a} [a S_1]' + S_2, \quad (\text{B12})$$

which can also be written as

$$\begin{aligned} \delta''_{2,t} + \frac{2}{\tau} \delta'_{2,t} - \frac{6}{\tau^2} \delta_{2,t} &= -\frac{1}{a} [a S_1]' + S_2 \\ &= t_{ij}^{(0)} \left\{ [3a' F' + a F''] x^i \partial^j + 2a' F' \frac{\partial^i \partial^j}{\nabla^2} + \frac{1}{a} [a(aF)']' \delta^{ij} \right\} \delta_{1,s}^{(0)}. \end{aligned} \quad (\text{B13})$$

The Green's function for this ODE, with the boundary conditions $\delta_{2,t}(0) = \delta'_{2,t}(0) = 0$, is

$$G(\tau, \tau') = \frac{1}{5} \left(\frac{\tau^2}{\tau'} - \frac{\tau'^4}{\tau^3} \right) \Theta(\tau - \tau'). \quad (\text{B14})$$

We then have

$$\begin{aligned} \int_0^\tau d\tau' G(\tau, \tau') a' F' &= \frac{2}{5} a(\tau) [F(\tau) - V(\tau)] \\ \int_0^\tau d\tau' G(\tau, \tau') a F'' &= \frac{1}{5} a(\tau) [-F(\tau) + 6V(\tau)] \\ \int_0^\tau d\tau' G(\tau, \tau') \frac{1}{a} [a(aF)']' &= a(\tau) \left[F(\tau) + \frac{3}{2} D_{\sigma 2}(\tau) \right]. \end{aligned} \quad (\text{B15})$$

Putting everything together, we obtain

$$\delta_{2,t}(\mathbf{x}, \tau) = t_{ij}^{(0)} \left\{ F(\tau) x^i \partial^j + \frac{4}{5} [F(\tau) - V(\tau)] \frac{\partial^i \partial^j}{\nabla^2} + \left[F(\tau) + \frac{3}{2} D_{\sigma 2}(\tau) \right] \delta^{ij} \right\} \delta_{1,s}(\mathbf{x}, \tau). \quad (\text{B16})$$

This agrees exactly with the result of the Lagrangian derivation, Eq. (38).

Appendix C: Numerical evaluation for Λ CDM

This section presents the equations used to numerically evaluate the tensor mode contribution for Λ CDM, i.e. including a cosmological constant in addition to matter and radiation. The numerical results are shown in Figs. 1–3. We have (assuming flatness)

$$H^2 = H_0^2 [\Omega_{\Lambda 0} + \Omega_{m0} a^{-3} + \Omega_{r0} a^{-4}] =: H_0^2 E^2(a), \quad (\text{C1})$$

where $a = 1$ today and

$$\Omega_{\Lambda 0} + \Omega_{m0} + \Omega_{r0} = 1. \quad (\text{C2})$$

The Ω_{X0} refer to fractions of the critical density today. The relation between a and the dimensionless conformal time $y = \tilde{H}_0 \tau$ needs to be solved numerically through

$$y(a) = \int_0^a \frac{da'}{a'^2 E(a')}. \quad (\text{C3})$$

However, deep in radiation and matter domination, we use the analytical result obtained when neglecting the Λ term in Eq. (C1):

$$y(a) = 2\Omega_{m0}^{-1/2} (\sqrt{a + a_{\text{eq}}} - \sqrt{a_{\text{eq}}}). \quad (\text{C4})$$

a. Linear solutions

Transforming the tensor mode equation to y , we obtain

$$D_h''(y) + 2f_H(y)D_h'(y) + \frac{k_L^2}{\tilde{H}_0^2} D_h(y) = 0 \quad (\text{C5})$$

$$\begin{aligned} f_H(y) &= a(y)E(a(y)) \\ D_h(0) &= 1; \quad D_h'(0) = 0, \end{aligned} \quad (\text{C6})$$

where for the remainder of this section primes stand for derivatives with respect to y . The Poisson equation is now

$$\nabla^2 \Phi = \frac{3}{2} \Omega_{m0} H_0^2 a^{-1}(y) \delta(y). \quad (\text{C7})$$

We define a linear growth factor $D_{1,s}$ for scalar perturbations through

$$\sigma_{1,s}(\mathbf{q}, \tau) = D_{1,s}(\tau) \sigma_{1,s}(\mathbf{q}, \tau_0), \quad (\text{C8})$$

which satisfies

$$D_{1,s}''(y) + f_H(y)D_{1,s}'(y) - \frac{3}{2} \Omega_{m0} a^{-1}(y) D_{1,s}(y) = 0 \quad (\text{C9})$$

with boundary conditions

$$D_{1,s}(0) = 0; \quad D_{1,s}(y_0) = 1. \quad (\text{C10})$$

In order to enforce these boundary conditions, we integrate the growth equation from some y_{min} deep in radiation domination, with initial conditions

$$D_{1,s}(y_{\text{min}}) = C; \quad D_{1,s}'(y_{\text{min}}) = \frac{C}{y_{\text{min}}}, \quad (\text{C11})$$

and adjust C so that $D_{1,s}(y_0) = 1$ where $a(y_0) = 1$.

b. Second order solution

In order to solve for $\sigma_{2,t}$, we transform Eq. (26) from τ to y , yielding

$$\begin{aligned} \sigma_{2,t}''(\mathbf{q}, y) + f_H(y)\sigma_{2,t}'(\mathbf{q}, y) - \frac{3}{2}\Omega_{m0}a^{-1}(y)\sigma_{2,t}(\mathbf{q}, y) &= \Sigma(\mathbf{q}, y) \\ \Sigma(\mathbf{q}, y) &= -\frac{1}{2}a^{-1}\frac{d}{dy}\left[a\frac{dD_h}{dy}\right]D_{1,s}(y)\Sigma_0(\mathbf{q}) \\ \Sigma_0(\mathbf{q}) &= \left(\frac{\partial^i\partial^j}{\nabla^2}\delta_{1,s}(\mathbf{q}, y_0)\right)h_{ij}^{(0)}. \end{aligned} \quad (\text{C12})$$

As before, we start integrating at y_{\min} where $k_L\tau_{\min} = k_L/\tilde{H}_0 y_{\min}$ is sufficiently small so that the right-hand side can be set to zero. The initial conditions for $\sigma_{2,t}$ are then

$$\sigma_{2,t}(y_{\min}) = 0; \quad \sigma_{2,t}'(y_{\min}) = 0. \quad (\text{C13})$$

We then solve Eq. (C12) numerically using a fourth-order Runge-Kutta scheme with adaptive step size.

Appendix D: Radiation domination

We now consider the case of dark matter during pure radiation domination (RD) in the Lagrangian treatment of Sec. III. In addition to clarifying the reason for the behavior of the tensor-scalar coupling shown in Fig. 2, these results are also used for the initial conditions of the numerical integration described in App. C. We have

$$\Omega_m = 0; \quad \mathcal{H}(a) = \tilde{H}_0 a^{-1}; \quad \tau = \tilde{H}_0^{-1} a; \quad \mathcal{H} = \tau^{-1}, \quad (\text{D1})$$

where \tilde{H}_0 is the Hubble constant at some reference time during RD where $a(\tau_0) = 1$.

1. Linear solutions

Since $\Omega_m = 0$, the q -divergence of the linearized scalar EOM becomes

$$\sigma_{1,s}''(\mathbf{q}, \tau) + \frac{1}{\tau}\sigma_{1,s}'(\mathbf{q}, \tau) = 0. \quad (\text{D2})$$

The growing mode corresponds to $\sigma_{1,s} \propto \ln \tau$, while the decaying mode is $\sigma_{1,s} = \text{const}$. In the following, we will again assume that the scalar perturbations have settled in the growing mode by the time when the tidal field t_{ij} becomes relevant. Since the growth is only logarithmic in τ rather than polynomial as in matter domination, this is a much stronger restriction.

We normalize the density perturbation $\delta_{1,s}(\mathbf{q}, \tau)$ to its value at horizon crossing $\mathcal{H}_* = 1/\tau_* = k_S$:

$$\delta_{1,s}(\mathbf{q}, \tau) = \ln(k_S\tau)\delta_{1,s}^{\text{H}}(\mathbf{q}) \quad (k_S\tau \gg 1), \quad (\text{D3})$$

which again is only valid if $k_S\tau \gg 1$. We then have

$$s_{1,s}^i(\mathbf{q}, \tau) = -\ln(k_S\tau)\frac{\partial_q^i}{\nabla_q^2}\delta_{1,s}^{\text{H}}(\mathbf{q}). \quad (\text{D4})$$

For the tidal field, Eqs. (20)–(23) are valid for a general expansion history.

2. Second-order solution

Again, since $\Omega_m = 0$, the source terms of the Poisson equation vanish, and Eq. (26) simplifies to

$$\sigma_{2,t}'' + \mathcal{H}\sigma_{2,t}' = -\mathbf{M}_{1,s}^{ij}t_{ij}, \quad (\text{D5})$$

where on the r.h.s. all contributions are evaluated at \mathbf{q} and τ . In reality, Ω_m is of course never exactly zero; thus, our results assume that t^i_i is not dramatically enhanced so that the prefactor of Ω_m sufficiently suppresses the first source term in Eq. (26) over the second one. We obtain

$$\begin{aligned} \sigma''_{2,t}(\mathbf{q}, \tau) + \frac{1}{\tau} \sigma'_{2,t}(\mathbf{q}, \tau) &= \Sigma(\mathbf{q}, \tau) \\ \Sigma(\mathbf{q}, \tau) &= \ln(k_S \tau) T(\tau) \Sigma_0(\mathbf{q}) = \ln(k_S \tau) T(\tau) \left(\frac{\partial^i \partial^j}{\nabla^2} \delta_{1,s}^H(\mathbf{q}) \right) t_{ij}^{(0)}. \end{aligned} \quad (\text{D6})$$

The growing and decaying modes are again $\sigma_{2,t} \propto \ln \tau$ and $\sigma_{2,t} \propto \text{const}$, respectively. The solution for this equation with the appropriate boundary conditions is given by

$$\sigma_{2,t}(\mathbf{q}, \tau) = \int_0^\tau d\tau' \tau' \ln\left(\frac{\tau}{\tau'}\right) \Sigma(\mathbf{q}, \tau'). \quad (\text{D7})$$

We then obtain using integration by parts (and $F(\tau \rightarrow 0) = 0$) to obtain

$$\begin{aligned} \sigma_{2,t}(\mathbf{q}, \tau) &= D_{\sigma 1}(\tau) \Sigma_0(\mathbf{q}) \\ D_{\sigma 1}(\tau) &= \int_{1/k_S}^\tau d\tau' \tau' \ln\left(\frac{\tau}{\tau'}\right) \ln(k_S \tau') T(\tau') \\ &= F(\tau) \ln(\tau k_S) - 2 \int_{1/k_S}^\tau \frac{d\tau'}{\tau'} F(\tau'). \end{aligned} \quad (\text{D8})$$

Thus,

$$\sigma_{2,t}(\mathbf{q}, \tau) = t_{ij}^{(0)} \left(\frac{\partial^i \partial^j}{\nabla^2} \delta_{1,s}(\mathbf{q}, \tau) \right) [F(\tau) - V^{\text{RD}}(\tau)], \quad (\text{D9})$$

where F is defined as before [Eq. (21)] and we have introduced

$$V^{\text{RD}}(\tau) = 2 [\ln k_S \tau]^{-1} \int_{1/k_S}^\tau \frac{d\tau'}{\tau'} F(\tau'). \quad (\text{D10})$$

As in Sec. III, the total contribution to the Eulerian density induced by the external tidal field is then given by Eq. (36), which yields for the second order part

$$\begin{aligned} \delta_{2,t}(\mathbf{x}, \tau) &= t_{ij}^{(0)} \left[- [F(\tau) - V^{\text{RD}}(\tau)] \frac{\partial^i \partial^j}{\nabla^2} + F(\tau) \left(\frac{\partial^i \partial^j}{\nabla^2} + \delta^{ij} + x^i \partial^j \right) \right] \delta_{1,s}(\mathbf{x}, \tau) \\ &= t_{ij}^{(0)} \left[V^{\text{RD}}(\tau) \frac{\partial^i \partial^j}{\nabla^2} + F(\tau) (\delta^{ij} + x^i \partial^j) \right] \delta_{1,s}(\mathbf{x}, \tau). \end{aligned} \quad (\text{D11})$$

This has very similar structure to the result in matter domination [Eq. (38)], the key difference being that the coefficient of the tidal term $\partial^i \partial^j / \nabla^2 \delta_{1,s}$ only involves the function V^{RD} rather than F .

3. Tensor modes

As in Sec. V, we have $F(\tau) = \frac{1}{2} [1 - D_h(\tau)]$, where in RD

$$D_h(\tau) = \frac{\sin k_L \tau}{k_L \tau}. \quad (\text{D12})$$

The function $V^{\text{RD}}(\tau)$ becomes

$$\begin{aligned} V^{\text{RD}}(\tau) &= [\ln k_S \tau]^{-1} \int_{k_L/k_S}^{k_L \tau} \frac{dx}{x} \left(1 - \frac{\sin x}{x} \right) \\ &= [\ln k_S \tau]^{-1} \left[\ln x - \text{Ci } x + \frac{\sin x}{x} \right]_{k_L/k_S}^{k_L \tau}. \end{aligned} \quad (\text{D13})$$

In the $k_L\tau \rightarrow \infty$ limit, $F(\tau) \rightarrow 1/2$ just as in matter domination. On the other hand, $V^{\text{RD}}(\tau)$ becomes

$$V^{\text{RD}}(\tau) \rightarrow [\ln k_S\tau]^{-1} \frac{\ln k_L\tau}{\ln k_S\tau} = \frac{\ln k_L\tau}{\ln k_L\tau + \ln(k_S/k_L)}. \quad (\text{D14})$$

For $k_L\tau \gg k_S/k_L$, V^{RD} logarithmically approaches 1 from below. Eq. (D11) becomes in this limit

$$\delta_{2,t}(\mathbf{x}, \tau) = h_{ij}^{(0)} \left[\frac{\ln k_L\tau}{\ln k_L\tau + \ln(k_S/k_L)} \frac{\partial^i \partial^j}{\nabla^2} + \frac{1}{2} x^i \partial^j \right] \delta_{1,s}(\mathbf{x}, \tau). \quad (\text{D15})$$

Thus, there is a non-zero second-order density for $k_L\tau \gg 1$ during radiation domination as well. Moreover, the only difference to the corresponding result for matter domination [Eq. (60)] is the numerical coefficient of the first term (2/5 in MD, order 1 in RD depending on $k_L\tau$), and the fact that it evolves logarithmically with τ .

Appendix E: Projection effects

We now derive the projection effect contribution to the observed local small-scale correlation function $\xi_\delta(\mathbf{r}, \tau|h)$. Here, \mathbf{r} and τ are the observationally inferred comoving separation and conformal time, respectively. We make no particular assumptions about the nature of the tracers which are used to measure the small-scale correlation function. We will only consider the tensor (or vector) case here, so that $h_{00} = 0 = h_{0i}$.

We begin with Eq. (45) in [15], which gives

$$\xi(\mathbf{r}, \tau|h) = \left[1 - a_{ij}(x)r^i \partial_r^j + \frac{1}{\mathcal{H}} \mathcal{T}(x) \partial_\tau + 2c(x) \right] \xi_F(\mathbf{r}; \tau) \quad (\text{E1})$$

where x is the inferred spacetime position of the center of the region in which the correlation function is measured, and $\xi_F(\mathbf{r}, \tau)$ is the correlation function in the local $\overline{\text{FNC}}$ frame. Further, a_{ij} is the distortion of the *standard ruler* defined by the correlation function, \mathcal{T} is the shift, in terms of the logarithm of the scale factor, between constant-proper-time and constant-observed-redshift surfaces, and c is the perturbation to the observed number density of the tracer induced by the tensor mode. We now consider each of these ingredients in turn. Note that each term in Eq. (E1) is gauge-invariant and in principle independently observable.

First, the ruler distortion is most naturally decomposed as

$$a_{ij} = \mathcal{C} \hat{n}_i \hat{n}_j + \hat{n}_{(i} \mathcal{P}_{j)k} \mathcal{B}^k + \mathcal{P}_{ik} \mathcal{P}_{jl} \mathcal{A}^{kl}, \quad (\text{E2})$$

where $\mathcal{P}^{ij} = \delta^{ij} - \hat{n}^i \hat{n}^j$ is the projection operator perpendicular to the line of sight \hat{n}^i . \mathcal{C} , \mathcal{B}_i , and \mathcal{A}_{ij} are the gauge-invariant ruler perturbations defined in [1], which, when specialized to a metric with $h_{00} = 0 = h_{0i}$ are given by

$$\begin{aligned} \mathcal{C} &= -\Delta \ln a - \frac{1}{2} h_{\parallel} - \partial_{\tilde{\chi}} \Delta x_{\parallel} \\ \mathcal{B}_i &= -\mathcal{P}_i^j h_{jk} \hat{n}^k - \hat{n}^k \partial_{\perp i} \Delta x_k - \partial_{\tilde{\chi}} \Delta x_{\perp i} \\ \mathcal{A}_{ij} &= -\Delta \ln a \mathcal{P}_{ij} - \frac{1}{2} \mathcal{P}_i^k \mathcal{P}_j^l h_{kl} - \frac{1}{2} (\mathcal{P}_{jk} \partial_{\perp i} + \mathcal{P}_{ik} \partial_{\perp j}) \Delta x^k. \end{aligned} \quad (\text{E3})$$

The displacements Δx^i , $\Delta \ln a$ are also given in [1] and again specializing to purely spatial metric perturbations

$$\Delta x_{\parallel} = -\frac{1}{2} \int_0^{\tilde{\chi}} d\chi h_{\parallel} - \frac{1 + \tilde{z}}{H(\tilde{z})} \Delta \ln a \quad (\text{E4})$$

$$\Delta x_{\perp}^i = \frac{1}{2} \mathcal{P}^{ij} (h_{jk})_o \hat{n}^k \tilde{\chi} - \int_0^{\tilde{\chi}} d\chi \left[\frac{\tilde{\chi}}{\chi} \mathcal{P}^{ij} h_{jk} \hat{n}^k - \frac{1}{2} (\tilde{\chi} - \chi) \partial_{\perp}^i h_{\parallel} \right]. \quad (\text{E5})$$

The perturbation to the scale factor at emission is given by

$$\Delta \ln a = \frac{1}{2} \int_0^{\tilde{\chi}} d\chi h'_{\parallel}. \quad (\text{E6})$$

In Eqs. (E3)–(E6), metric perturbations outside integrals are evaluated at the source, unless they are marked by a subscript o , in which case they are evaluated at the observer. Metric perturbations inside integrals are evaluated on the past lightcone in the background, i.e. at

$$x^i = \hat{n}^i \chi; \quad x^0 = \tau_o - \chi, \quad (\text{E7})$$

where τ_o is the conformal time at observation. Primes denote derivatives with respect to τ , and $\tilde{\chi} \equiv \bar{\chi}(\tilde{z})$ where $\bar{\chi}(z)$ is the comoving distance-redshift relation in the background and \tilde{z} is the observed redshift. Further,

$$\partial_{\perp}^i = \mathcal{P}^{ij} \partial_j; \quad h_{\parallel} = h_{ij} \hat{n}^i \hat{n}^j. \quad (\text{E8})$$

The decomposition given by Eq. (E2) allows us to easily derive the distortions along and perpendicular to the line of sight in 3D space. However, writing the expressions in Cartesian form leads to more compact expressions. Using that, for an arbitrary symmetric tensor a_{ij} ,

$$a_{ij} = a_{\parallel} \hat{n}_i \hat{n}_j + 2 \hat{n}_{(i} \mathcal{P}_{j)}^k \hat{n}^l a_{kl} + \mathcal{P}_i{}^k \mathcal{P}_j{}^l a_{kl}, \quad (\text{E9})$$

Eq. (E2) becomes

$$a_{ij} = -\Delta \ln a \delta_{ij} - \frac{1}{2} h_{ij} - \partial_{(i} \Delta x_{j)} = -\frac{1}{2} \int_0^{\tilde{\chi}} d\chi h'_{\parallel} \delta_{ij} - \frac{1}{2} h_{ij} - \partial_{(i} \Delta x_{j)}. \quad (\text{E10})$$

The first equality can also be read off directly from Eq. (30) in [1], when setting $v^i = 0$. Note however, that as discussed in [1, 32], the derivative along the line of sight is really a derivative with respect to observed redshift, i.e. along the past light cone:

$$\hat{n}^i \partial_i \Delta x^k \equiv \frac{\partial}{\partial \tilde{\chi}} \Delta x^k = \left(\frac{d\bar{\chi}(\tilde{z})}{d\tilde{z}} \right)^{-1} \frac{\partial}{\partial \tilde{z}} \Delta x^k. \quad (\text{E11})$$

This subtlety is somewhat glossed over in the notation Eq. (E10), which does not make explicit the fundamental difference between line-of-sight and transverse directions.

We further need \mathcal{T} , which was derived in [25] and is given in our case by

$$\mathcal{T} = \Delta \ln a = \frac{1}{2} \int_0^{\tilde{\chi}} d\chi h'_{\parallel}. \quad (\text{E12})$$

Finally, the observed fractional number density perturbation of tracers induced by tensor modes was derived in [26] (note that δz in that paper is equal to $\Delta \ln a$ defined above). It is given by

$$c = b_e \Delta \ln a + \partial_i \Delta x^i + \mathcal{Q} \mathcal{M}_T, \quad (\text{E13})$$

where the magnification induced by a tensor mode is

$$\mathcal{M}_T = -2\Delta \ln a + \frac{1}{2} h_{\parallel} - \frac{2\Delta x_{\parallel}}{\tilde{\chi}} + 2\hat{\kappa}, \quad (\text{E14})$$

and the convergence is

$$\hat{\kappa} \equiv -\frac{1}{2} \partial_{\perp i} \Delta x^i_{\perp} = \frac{5}{4} h_{\parallel o} - \frac{1}{2} h_{\parallel} - \frac{1}{2} \int_0^{\tilde{\chi}} d\chi \left[h'_{\parallel} + \frac{3}{\chi} h_{\parallel} \right] - \frac{1}{4} \nabla_{\Omega}^2 \int_0^{\tilde{\chi}} d\chi \frac{\tilde{\chi} - \chi}{\tilde{\chi} \chi} h_{\parallel}. \quad (\text{E15})$$

Here $\nabla_{\Omega}^2 = \tilde{\chi}^2 \nabla_{\perp}^2$ denotes the Laplacian on the unit 2-sphere. The Jacobian in Eq. (E13) is then given by

$$\partial_i \Delta x^i = \partial_{\tilde{\chi}} \Delta x_{\parallel} + \frac{2\Delta x_{\parallel}}{\tilde{\chi}} - 2\hat{\kappa}. \quad (\text{E16})$$

Note again the subtlety in the Cartesian notation. The number density modulation is governed by two tracer-dependent parameters: the magnification bias parameter \mathcal{Q} , given in the simplest case of a sharp flux-limited survey by $\mathcal{Q} = -d \ln \bar{n}_g / d \ln f_{\text{cut}}$; and the parameter b_e , which quantifies the redshift evolution of the comoving number density of tracers through

$$b_e \equiv \left. \frac{d \ln(a^3 \bar{n}_g)}{d \ln a} \right|_{\tilde{z}} = -(1 + \tilde{z}) \left. \frac{d \ln(a^3 \bar{n}_g)}{dz} \right|_{\tilde{z}}. \quad (\text{E17})$$

Putting everything together, the observed local two-point correlation function becomes

$$\xi(\mathbf{r}, \tau|h) = \left[1 + \left\{ \frac{1}{2} \int_0^{\bar{\chi}} d\chi h'_{\parallel} \delta_{ij} + \frac{1}{2} h_{ij} + \partial_{(i} \Delta x_{j)} \right\} r^i \partial_r^j + \frac{1}{2\mathcal{H}} \int_0^{\bar{\chi}} d\chi h'_{\parallel} \partial_{\tau} \right. \\ \left. + 2 \left\{ \frac{b_e}{2} \int_0^{\bar{\chi}} d\chi h'_{\parallel} + \partial_i \Delta x^i + \mathcal{Q} \mathcal{M}_T \right\} \right] \xi_F(\mathbf{r}; \tau). \quad (\text{E18})$$

-
- [1] F. Schmidt and D. Jeong, *Phys. Rev. D* **86**, 083527 (2012), 1204.3625.
- [2] P. Creminelli, A. Perko, L. Senatore, M. Simonović, and G. Trevisan, *JCAP* **11**, 015 (2013), 1307.0503.
- [3] P. Creminelli, J. Gleyzes, M. Simonović, and F. Vernizzi (2013), 1311.0290.
- [4] P. Creminelli, J. Noreña, M. Simonović, and F. Vernizzi (2013), 1309.3557.
- [5] N. Bartolo, S. Matarrese, O. Pantano, and A. Riotto, *Class.Quant.Grav.* **27**, 124009 (2010), 1002.3759.
- [6] S. B. Giddings and M. S. Sloth, *Phys.Rev.* **D84**, 063528 (2011), 1104.0002.
- [7] M. Peloso and M. Pietroni, *JCAP* **5**, 031 (2013), 1302.0223.
- [8] A. Kehagias and A. Riotto, *Nuclear Physics B* **873**, 514 (2013), 1302.0130.
- [9] P. Valageas, *ArXiv e-prints* (2013), 1311.4286.
- [10] A. Kehagias, J. Noreña, H. Perrier, and A. Riotto, *ArXiv e-prints* (2013), 1311.0786.
- [11] A. Kehagias, H. Perrier, and A. Riotto, *ArXiv e-prints* (2013), 1311.5524.
- [12] K. W. Masui and U.-L. Pen, *Physical Review Letters* **105**, 161302 (2010), 1006.4181.
- [13] F. Schmidt and D. Jeong, *Phys. Rev. D* **86**, 083513 (2012), 1205.1514.
- [14] L. Dai, D. Jeong, and M. Kamionkowski, *ArXiv e-prints* (2013), 1306.3985.
- [15] E. Pajer, F. Schmidt, and M. Zaldarriaga, *ArXiv e-prints* (2013), 1305.0824.
- [16] D. Jeong and M. Kamionkowski, *ArXiv e-prints* (2012), 1203.0302.
- [17] U.-L. Pen, R. Sheth, J. Harnois-Deraps, X. Chen, and Z. Li, *ArXiv e-prints* (2012), 1202.5804.
- [18] P. J. E. Peebles, *Astrophys. J.* **155**, 393 (1969).
- [19] P. Catelan, M. Kamionkowski, and R. D. Blandford, *MNRAS* **320**, L7 (2001), arXiv:astro-ph/0005470.
- [20] C. M. Hirata and U. Seljak, *Phys. Rev. D* **70**, 063526 (2004), astro-ph/0406275.
- [21] F. K. Manasse and C. W. Misner, *Journal of Mathematical Physics* **4**, 735 (1963).
- [22] T. Baldauf, U. Seljak, L. Senatore, and M. Zaldarriaga, *ArXiv e-prints* (2011), 1106.5507.
- [23] F. Bernardeau, S. Colombi, E. Gaztañaga, and R. Scoccimarro, *Phys. Rep.* **367**, 1 (2002), arXiv:astro-ph/0112551.
- [24] D. Baumann, A. Nicolis, L. Senatore, and M. Zaldarriaga, *JCAP* **1207**, 051 (2012), 1004.2488.
- [25] D. Jeong and F. Schmidt, *ArXiv e-prints* (2013), 1305.1299.
- [26] D. Jeong and F. Schmidt, *Phys. Rev. D* **86**, 083512 (2012), 1205.1512.
- [27] S. Dodelson, E. Rozo, and A. Stebbins, *Physical Review Letters* **91**, 021301 (2003), arXiv:astro-ph/0301177.
- [28] C. M. Hirata, R. Mandelbaum, M. Ishak, U. Seljak, R. Nichol, K. A. Pimbblet, N. P. Ross, and D. Wake, *MNRAS* **381**, 1197 (2007), astro-ph/0701671.
- [29] T. Okumura and Y. P. Jing, *Astrophys. J. Lett.* **694**, L83 (2009), 0812.2935.
- [30] J. Blazek, M. McQuinn, and U. Seljak, *JCAP* **5**, 10 (2011), 1101.4017.
- [31] L. Book, M. Kamionkowski, and F. Schmidt, *ArXiv e-prints* (2011), 1112.0567.
- [32] D. Jeong, F. Schmidt, and C. M. Hirata, *Phys. Rev. D* **85**, 023504 (2012), 1107.5427.